CHAPTER IV
RESULTS AND DISCUSSION

4.1 Selection of Appropriate Methods for Catalyst Preparation

As described in chapter III, the catalyst samples were prepared by coprecipitation and deposition-precipitation methods by varying the metal loading. The required amounts of gold loaded were 0.5 wt.%, 1.0 wt.%, and 1.5 wt.%Au. The actual amounts of gold loaded on three different supports were analyzed by using AAS (atomic absorption spectrophotometer). To determine the appropriate methods for gold catalyst preparation on three different supports, some gold catalysts were prepared using two preparation methods at three different calcination temperature and then the catalyst samples prepared were measured their BET surface areas. Table 4.1 shows the BET surface areas of the catalyst samples prepared. As shown in Table 4.1, the BET surface area strongly depends on both calcination temperature and preparation method. It was found that coprecipitation method could provide relatively high surface areas for preparing Au/NiO and Au/Y_2O_3 but it gave considerably low surface areas for preparing Au/MnO_2. Meanwhile, deposition-precipitation method gave considerably high surface areas for preparing Au/MnO_2. In addition, the results obtained agree with the work of Haruta *et al.* (1989) that coprecipitation method was useful for the preparation of powder catalysts, and especially for Au/NiO, Au/α-FeO_2, Au/Co_3O_4, and $Au/Be(OH)_2$ whereas the deposition-coprecipitation method was appropriate for gold supported on MnO_2 since an important requirement for deposition-precipitation method is that the support materials should have high specific surface areas, preferably larger than 50 m^2/g (Haruta, 1997c). Therefore, coprecipitation method was selected for preparing both Au/NiO and Au/Y_2O_3

while Au/MnO_2 was prepared by using deposition-precipitation method. This selection was to obtain relatively high surface areas of the catalysts prepared since oxidative reactions are generally dependent on the surface area of catalysts.

Table 4.1 BET surface areas of catalysts prepared under different conditions

Samples	Preparation method	BET surface area of catalysts at different calcination temperature (m^2/g)		
		300°C	400°C	500°C
0.12 wt.% Au/NiO	CO	235.5	77.28	32.46
0.35 wt.%Au/MnO_x	CO	12.13	13.95	11.31
0.18 wt.%Au/Y_2O_3	CO	40.57	39.51	81.91
0.5 wt%Au/NiO	DP	-	0.4947	-
0.48 wt%Au/MnO_2	DP	110.0	96.56	75.31
0.5 wt%Au/Y_2O_3	DP	-	0.945	-

Note: CO indicates coprecipitation method

DP indicates deposition-precipitation method

4.2 Determination of Actual Gold Loadings in Prepared Catalysts

The actual amounts of gold loadings of all catalysts prepared were determined by atomic absorption spectroscopy as described earlier in Chapter III. Table 4.2 shows the comparison between the prepared values and the actual values of gold contents in all gold catalysts prepared using different supports and two different preparation methods. Surprisingly, it was found that significant losses of gold occurred during the preparation procedures. This was due to the hygroscopic property of hydrogen tetrachloroaurate trihydrate used

as a precursor for gold catalysts. Moreover, deposition-precipitation method gave relatively much higher gold content than coprecipitation method.

Table 4.2 The actual amounts of gold loadings of prepared catalysts

Support	Calcination temperature (°C)	Wt.% of gold content		
		Prepared value	Actual value	Average actual value
NiO	300	0.5 wt.%	0.12	0.12
	400		0.12	
	500		0.13	
	300	1.0 wt.%	0.22	0.22
	400		0.22	
	500		0.24	
	300	1.5 wt.%	1.75	1.74
	400		1.70	
	500		1.77	
MnO_2	300	0.5 wt.%	0.48	0.48
	400		0.51	
	500		0.47	
	300	1.0 wt.%	0.92	0.95
	400		0.97	
	500		0.96	
	300	1.5 wt.%	1.34	1.40
	400		1.45	
	500		1.40	
Y_2O_3	300	0.5 wt.%	0.18	0.18
	400		0.19	
	500		0.18	
	300	1.0 wt.%	0.21	0.23
	400		0.22	
	500		0.25	
	300	1.5 wt.%	0.49	0.58
	400		0.57	
	500		0.67	

4.3 BET Surface Areas of Prepared Catalysts

The BET surface areas of the gold-doped oxide catalysts prepared at different of gold loadings, different calcination temperatures and using different preparation methods and three types of supports are shown in Tables 4.3-4.6. It can be seen clearly that BET surface area of Au/NiO appreciably decreased drastically with increasing calcination temperature but increased slightly with increasing gold loading. Interestingly, for the highest gold loading of 1.74 wt.% an increase in its BET surface area was not so high as compared to the BET surface area at loading of 0.22wt.%. It might be due to the coagulation of Au particles. For calcination temperature of 400°C, BET surface area in the same order of magnitude of that of Au/NiO (116 m^2/g) calcined at the same temperature in the work of Haruta *et al.* (1989). For Au/MnO_2, the gold loading did not affect the BET surface area but it showed a significant effect of calcination temperature on the surface area. When calcination temperature increased, the BET surface area slightly decreased. This was due to a reduction of the BET surface area of pure MnO_2 by itself. For Au/Y_2O_3 catalysts, the surface area increased slightly with increasing calcination temperature but it decreased substantially when gold loading increased in the studied range. In conclusion, the surface areas of gold catalysts prepared in this study depended on both calcination temperature and type of support used.

Table 4.3 BET surface areas of Au/NiO catalysts prepared by coprecipitation Method

Calcination temperature(°C)	**Surface area at different gold loading (m^2/g)**			
	0.00 wt.%	**0.12 wt.%**	**0.22 wt.%**	**1.74 wt.%**
300	224.2	235.5	257.03	279.8
400	82.49	77.28	109.3	114.75
500	32.45	32.46	38.52	39.10

Table 4.4 BET surface areas of Au/MnO_2 catalysts prepared by deposition-precipitation method

Calcination temperature(°C)	Surface area at different gold loading (m^2/g)			
	0.00 wt.%	**0.48 wt.%**	**0.95 wt.%**	**1.40 wt.%**
300	100.2	110.0	109.65	108.65
400	88.05	96.56	95.06	91.23
500	76.19	75.31	74.43	76.29

Table 4.5 BET surface areas of Au/Y_2O_3 catalysts prepared by coprecipitation method

Calcination temperature(°C)	Surface area at different gold loading (m^2/g)			
	0.00 wt.%	**0.18 wt.%**	**0.23 wt.%**	**0.58 wt.%**
300	59.07	40.57	33.57	24.9
400	60.92	39.51	36.04	26.26
500	71.07	81.91	38.46	37.81

4.4 X-ray Diffraction Analysis (XRD)

X-ray diffraction analysis was carried out for all catalysts. The XRD patterns for the different gold supported catalysts are shown in Figures 4.1-4.18. By comparing Figures 4.1-4.3, the XRD patterns of Au/NiO catalysts for all doping levels look similar when they were calcined at the same temperature. It can be noticed that Au/NiO catalyst calcined at 300°C had broader peaks than those calcined at 400°C and 500°C. It can be implied that NiO crystals calcined at 300°C were smaller than those calcined at 400°C and 500°C because the crystallite size is inversely proportional to the peak width. As the crystals get smaller and smaller, the XRD peaks get broader and

broader and eventually are undetectable. It was interesting that for a series of 0.12 wt.% Au/NiO and 0.22 wt.% Au/NiO (Figure 4.1and Figure 4.2), no any peak of gold crystal was detected. It might be assumed that the amount of gold was so little that it was over the limitation on the performance of XRD instrument to detect a trace amount of gold crystals. However, for the highest doping level of 1.74 wt.% Au four peaks of gold crystal appear at about 38.2 , 44.4, 64.6, and 78° (2θ) as shown in Figure 4.3. This result is also confirmed by the previous works (Haruta *et al.,* 1989; and Sukjit, 1999). Figures 4.4-4.6 show the comparison of XRD patterns of Au/NiO under different gold loading at any given calcination temperature. It was clearly seen that the shapes of peaks for all metal loadings at any given calcination temperature, the patterns and the peak intensities of all patterns are all nearly the same. It could be concluded that it was not gold loading but calcination temperature affecting the crystalline structure of both gold and NiO.

The XRD patterns of a series of Au/MnO_2 are shown in Figures 4.7-4.12. Figures 4.7-4.9 show the effect of calcination temperature at different gold loading on the crystalline structures of gold particles and MnO_2. It could be noticed that at any given gold loading, the peak of gold for calcination temperature of 400°C at 2θ about 38.2 degree was more obvious and sharper than those calcined at other temperatures. It can be implied that uniform gold crystals on MnO_2 support are obtained when calcined at 400°C. For the effect of metal loading, (Figures 4.10-4.12), it is evident that a higher gold loading gave a higher intensity.

As be shown in Figures 4.13-4.15, for any given gold loading, the XRD patterns of Au/Y_2O_3 catalysts calcined at 300°C and 400°C are similar but they are clearly different from that calcined at 500°C. It can be implied that the structure of yttrium oxide might be perfectly transformed to Y_2O_3 when calcination temperature was up to 500°C whereas the temperatures of 300°C and 400°C were not adequately high enough to perfectly transform

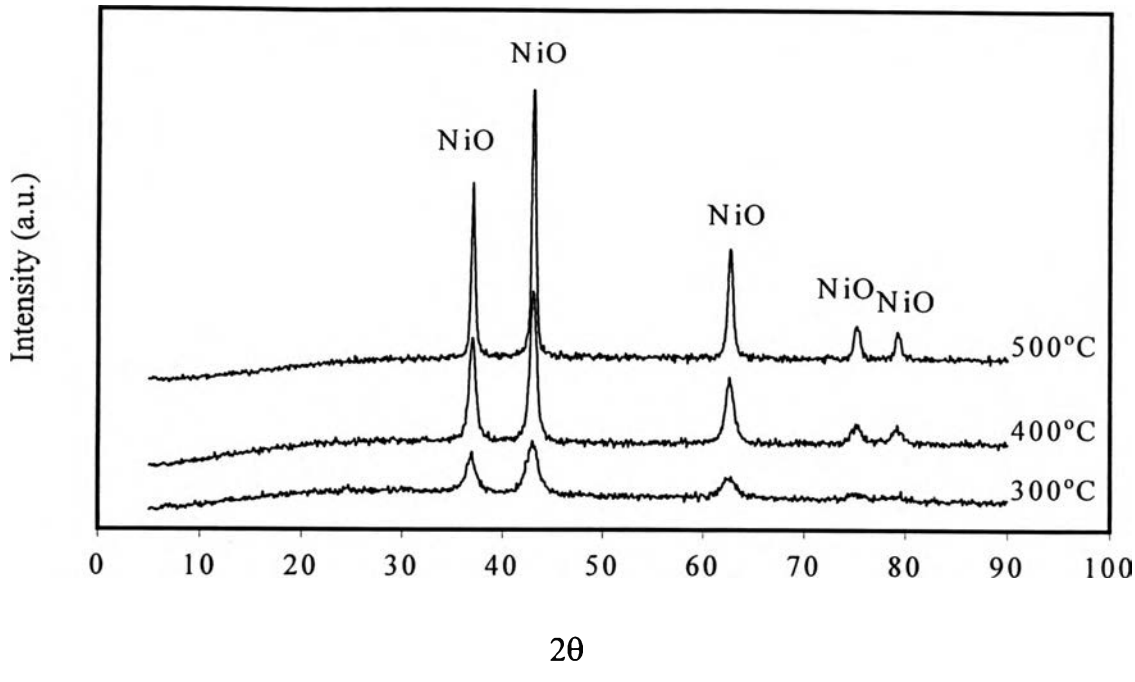

Figure 4.1 XRD patterns of a series of 0.12 wt.% Au/NiO calcined at different temperatures

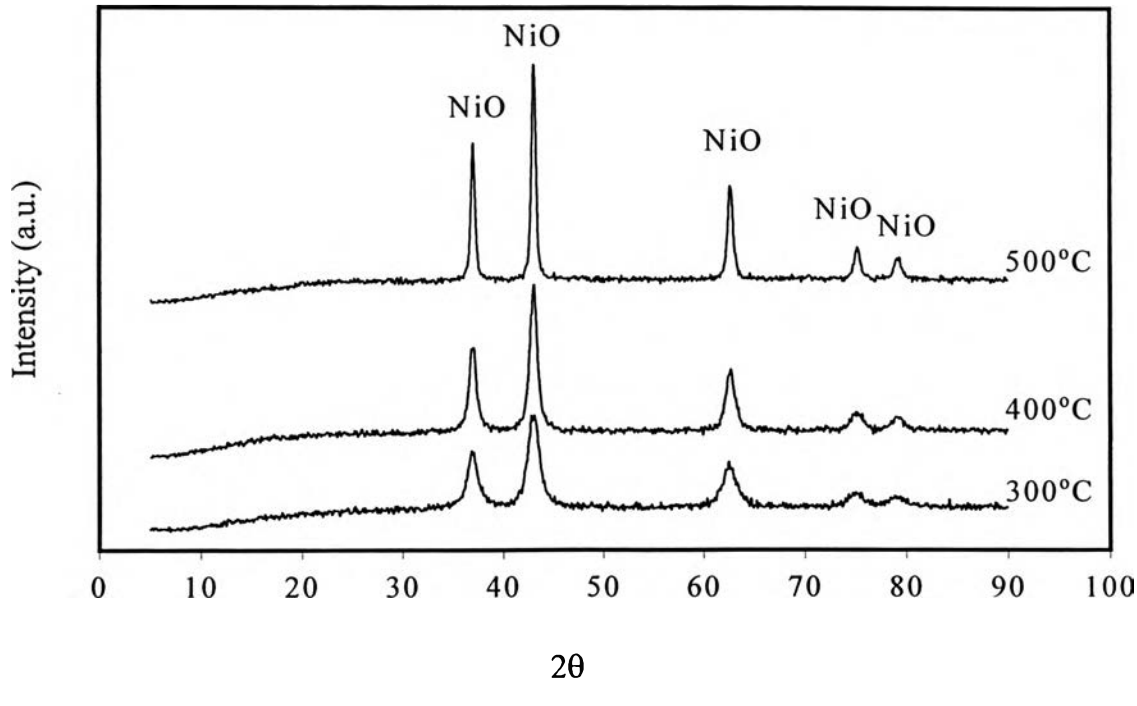

Figure 4.2 XRD patterns of a series of 0.22 wt.% Au/NiO calcined at different temperatures

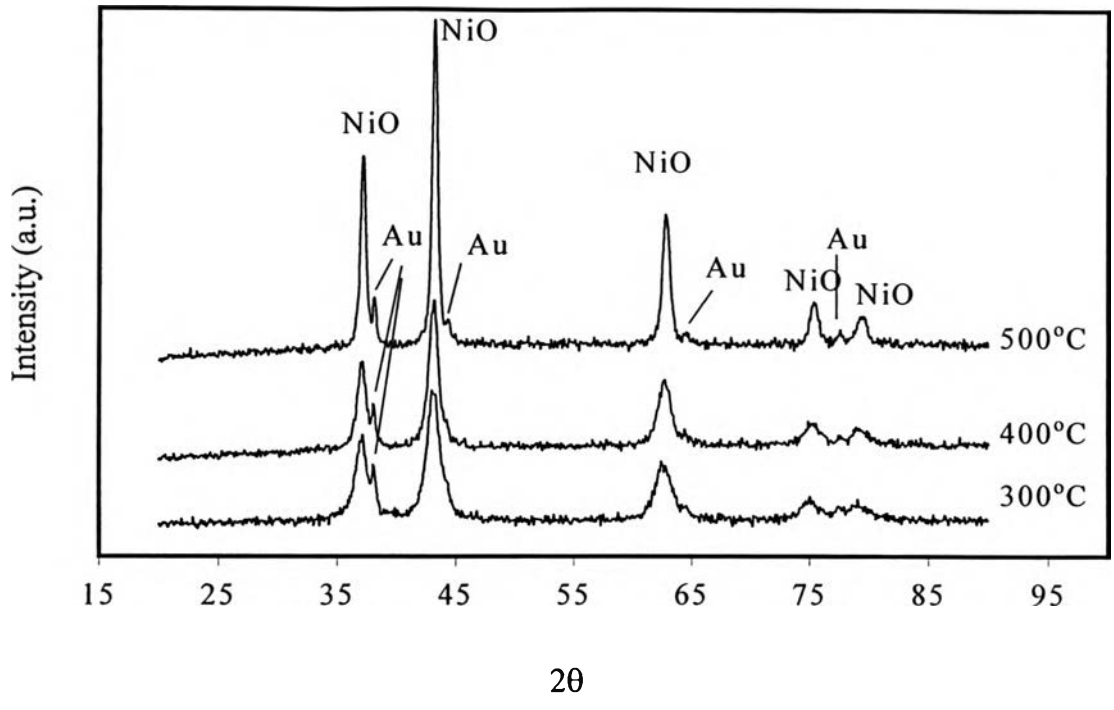

Figure 4.3 XRD patterns of a series of 1.74 wt.% Au/NiO calcined at different temperatures

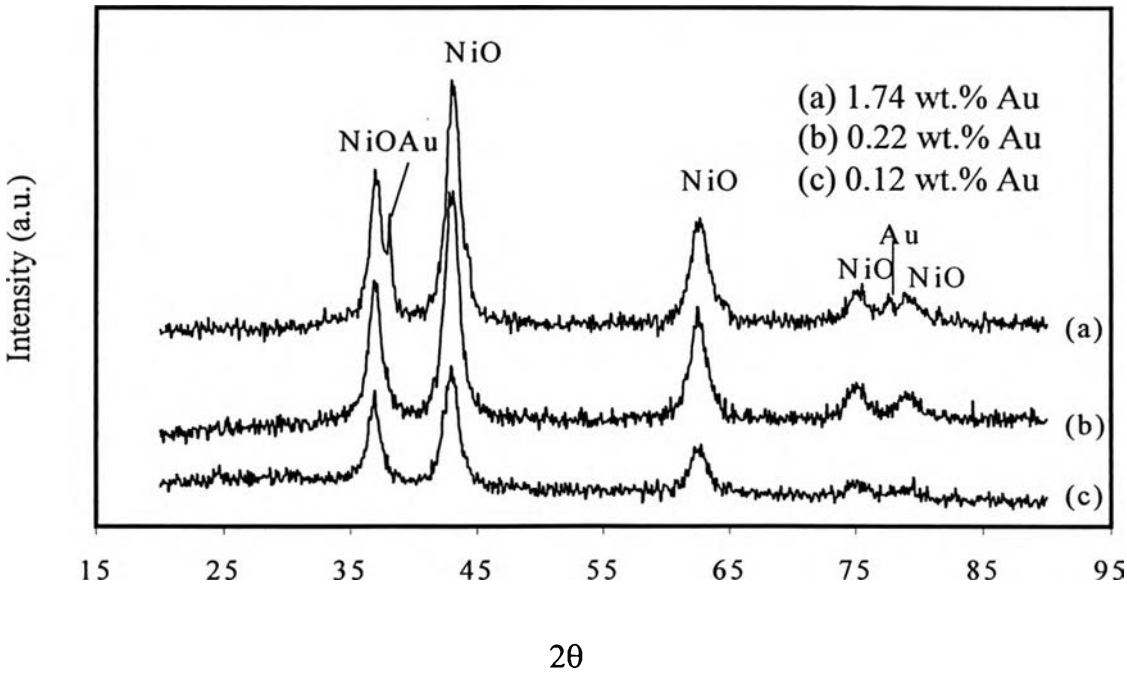

Figure 4.4 XRD patterns of a series of Au/NiO having different gold loadings and calcined at 300°C

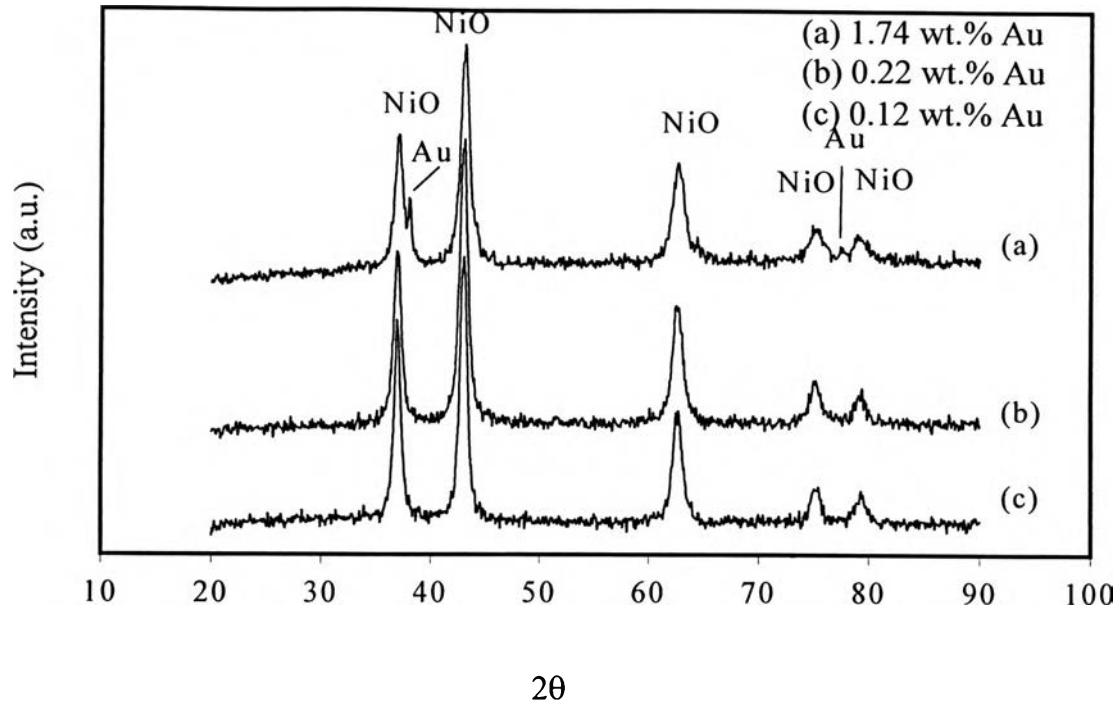

Figure 4.5 XRD patterns of a series of Au/NiO having different gold loadings and calcined at 400°C

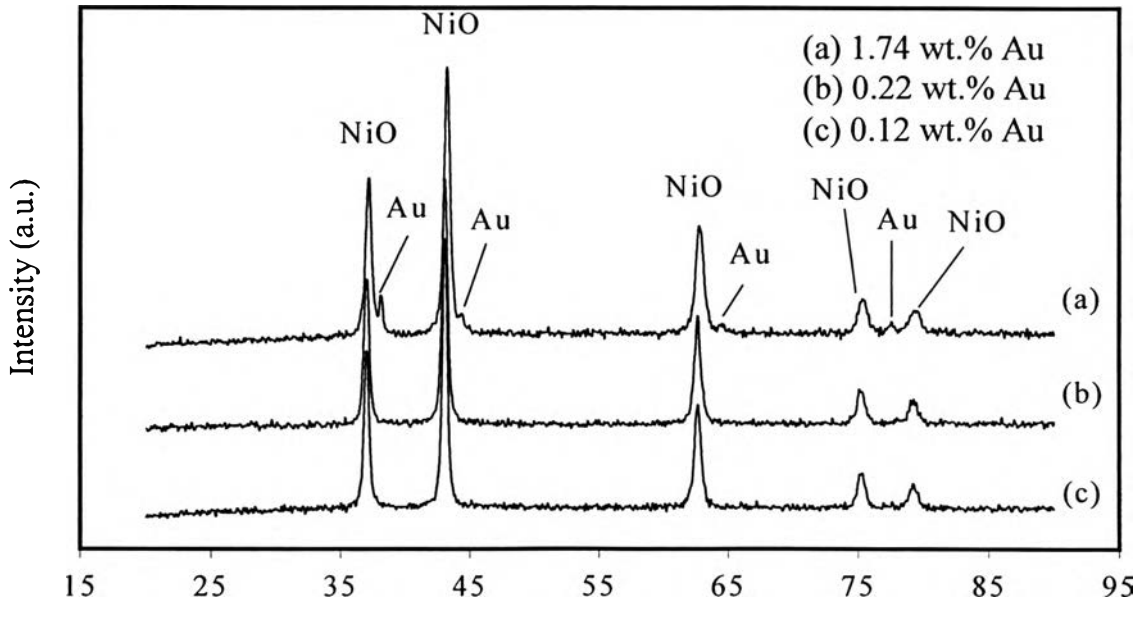

Figure 4.6 XRD patterns of a series of Au/NiO having different gold loadings and calcined at 500°C

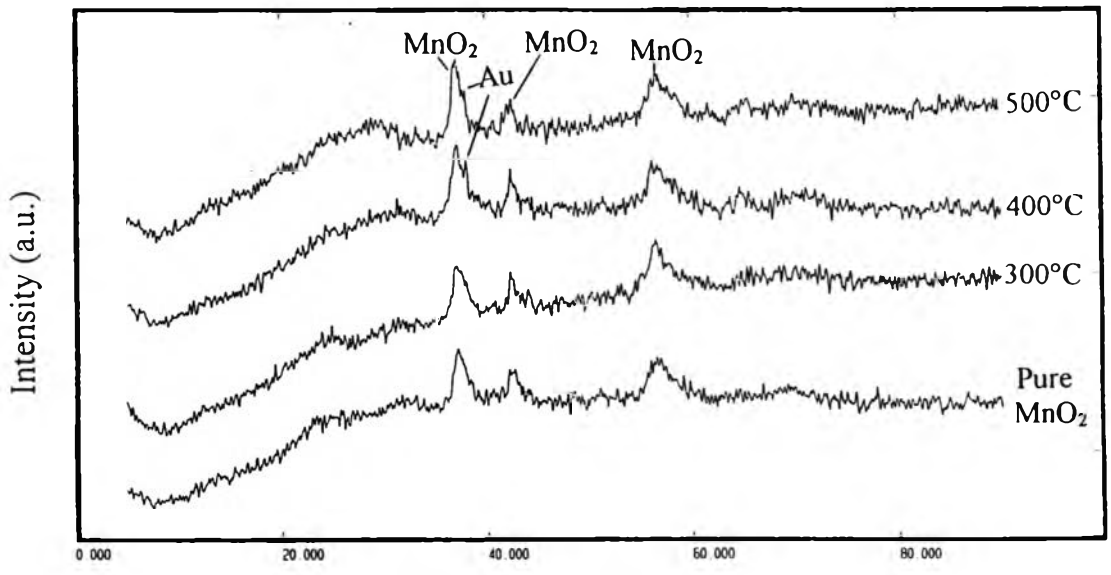

Figure 4.7 XRD patterns of a series of 0.48 wt.% Au/MnO_2 calcined at different temperatures

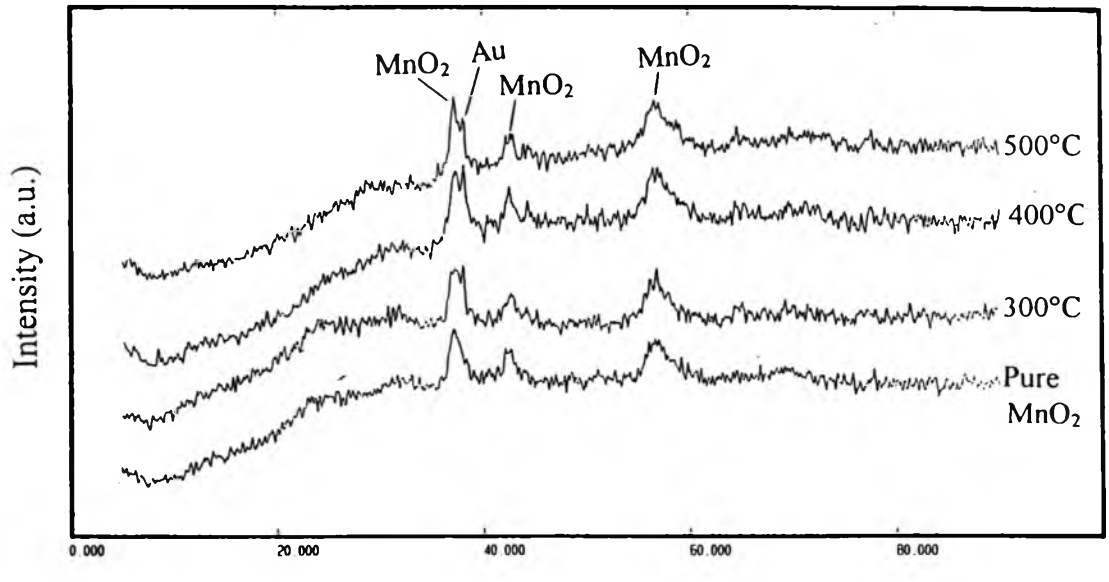

Figure 4.8 XRD patterns of a series of 0.95 wt.% Au/MnO_2 calcined at different temperatures

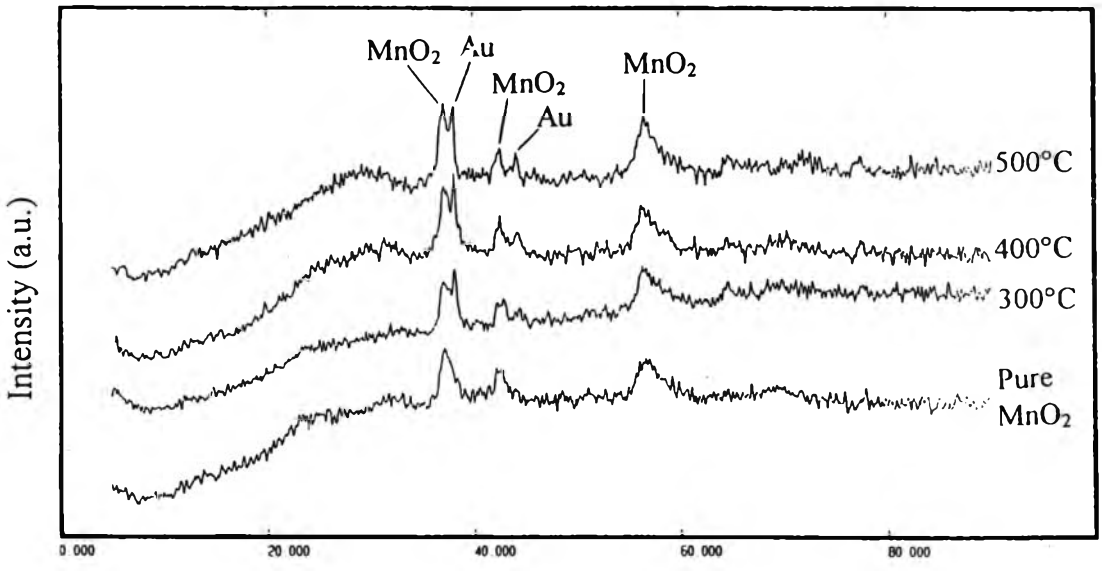

Figure 4.9 XRD patterns of a series of 1.40 wt.% Au/MnO_2 calcined at different temperatures

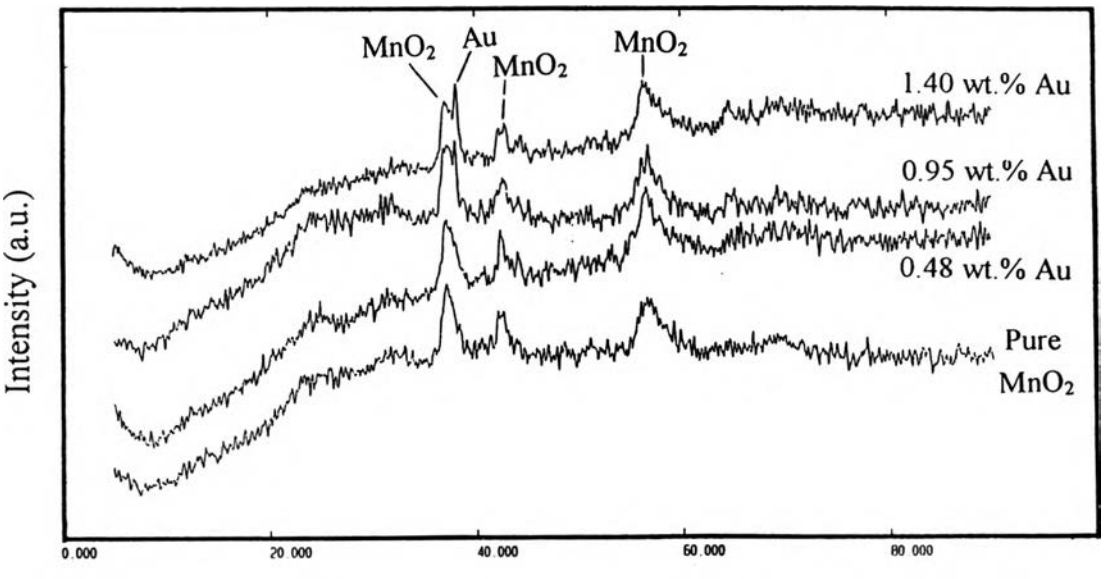

Figure 4.10 XRD patterns of a series of Au/MnO_2 having different gold loadings and calcined at 300°C

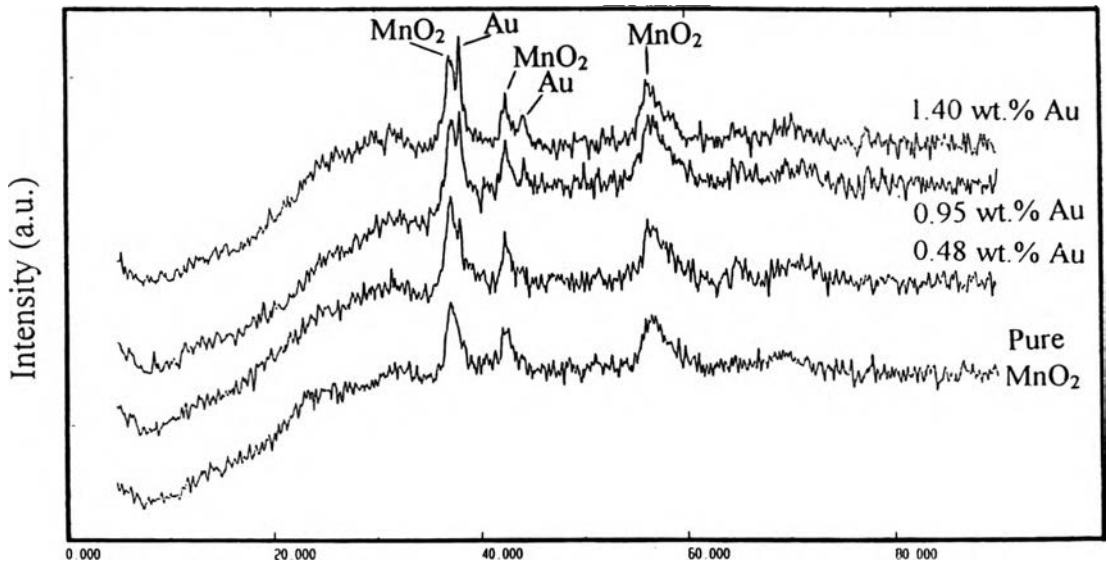

Figure 4.11 XRD patterns of a series of Au/MnO_2 having different gold loadings and calcined at 400°C

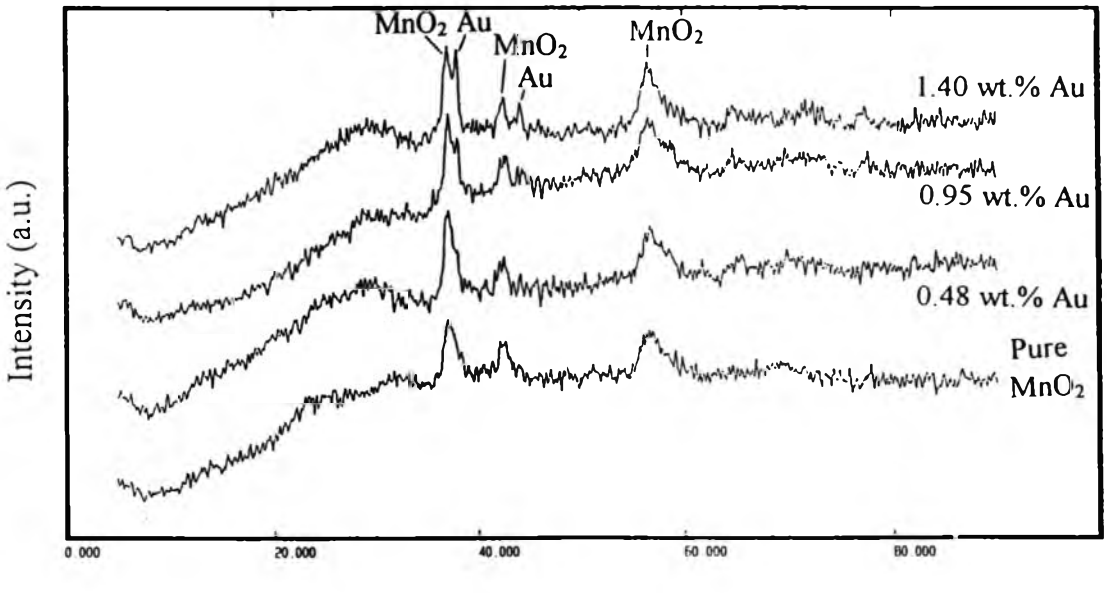

Figure 4.12 XRD patterns of a series of Au/MnO_2 having different gold loadings and calcined at 500°C

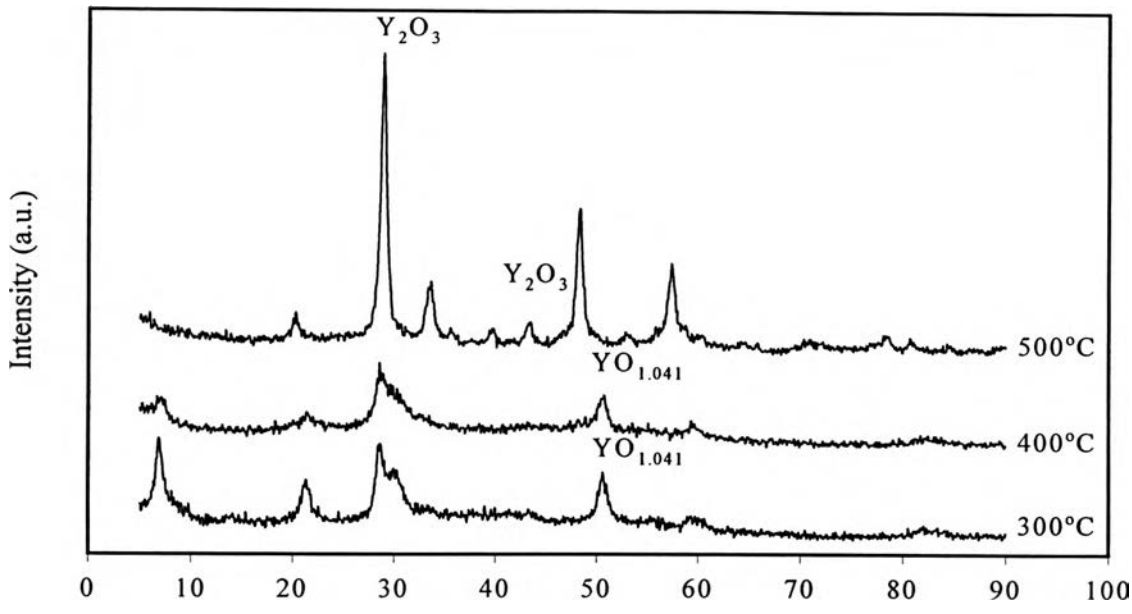

Figure 4.13 XRD patterns of a series of 0.18 wt.% Au/Y_2O_3 calcined at different temperatures

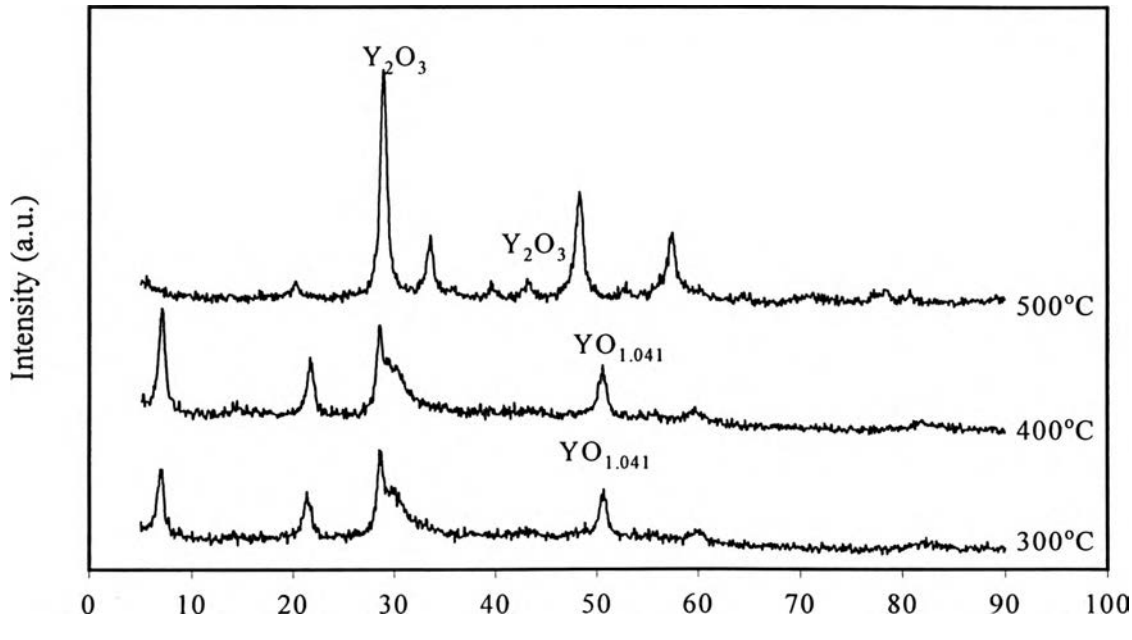

Figure 4.14 XRD patterns of a series of 0.23 wt.% Au/Y_2O_3 calcined at different temperatures

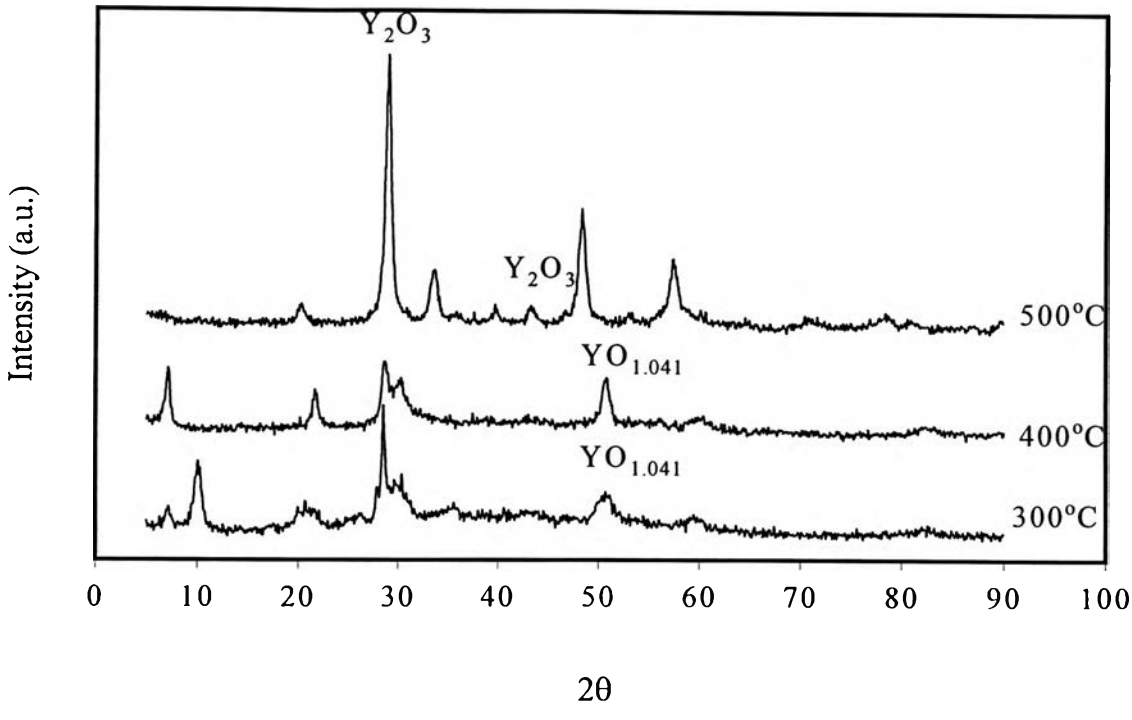

Figure 4.15 XRD patterns of a series of 0.58 wt.% Au/Y_2O_3 calcined at different temperatures

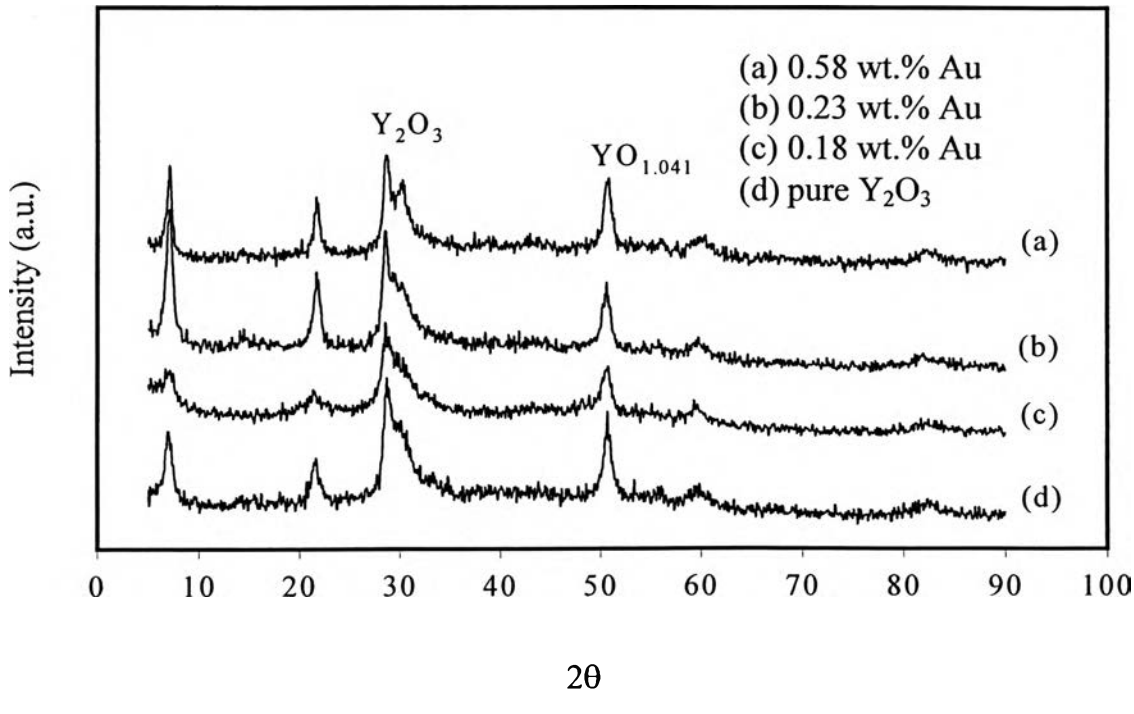

Figure 4.16 XRD patterns of a series of Au/Y_2O_3 having different gold loadings and calcined at 300°C

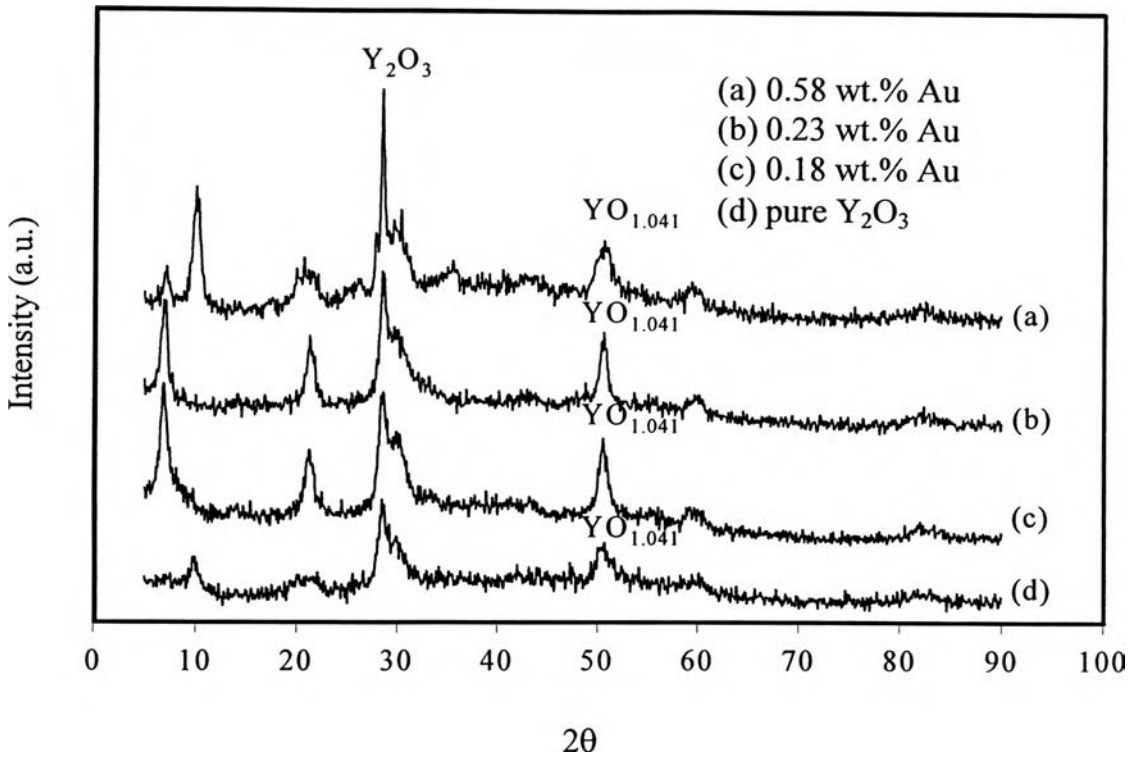

Figure 4.17 XRD patterns of a series of Au/Y_2O_3 having different gold loadings and calcined at 400°C

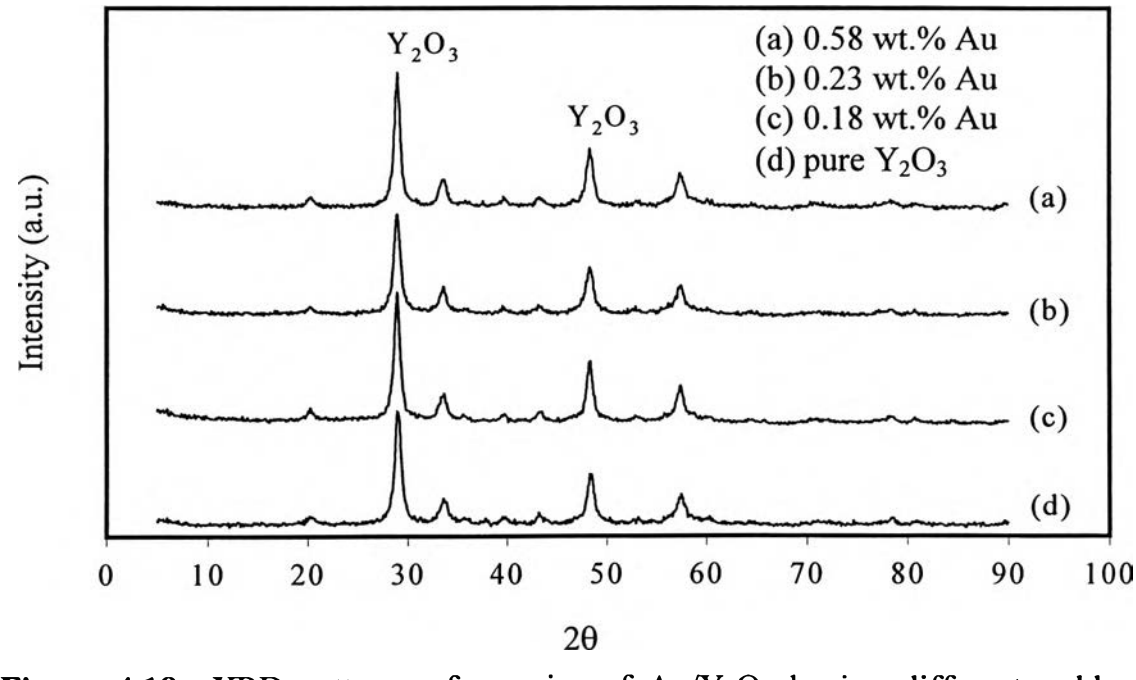

Figure 4.18 XRD patterns of a series of Au/Y_2O_3 having different gold loadings and calcined at 500°C

yttrium hydroxide to Y_2O_3. This conclusion can be furthermore confirmed by identification of the one peak appearing at 2θ about 51 degree which is $YO_{1.041}$ at the calcination temperatures of 300°C and 400°C. Furthermore, this hypothesis is also confirmed by the work of Lee and Tak (1999). They showed that $Y(OH)_3$ phase transformed to α-$Y(OH)_3$ at about 400°C, and then Y_2O_3 above 450°C. In addition, no any peak of gold was detected. It is believed that the small amount of gold might be too little or the crystal size of gold was not big enough to be detected by XRD.

4.5 Morphology of prepared catalysts

TEM micrographs of all gold-supported catalysts studied are shown in Figures 4.19-4.45. It was found that the morphology of the catalysts changed with calcination temperature. As can be seen in Figure 4.19 - 4.21 , the TEM

Figure 4.19 TEM micrograph of 0.12 wt.% Au/NiO calcined at 300°C

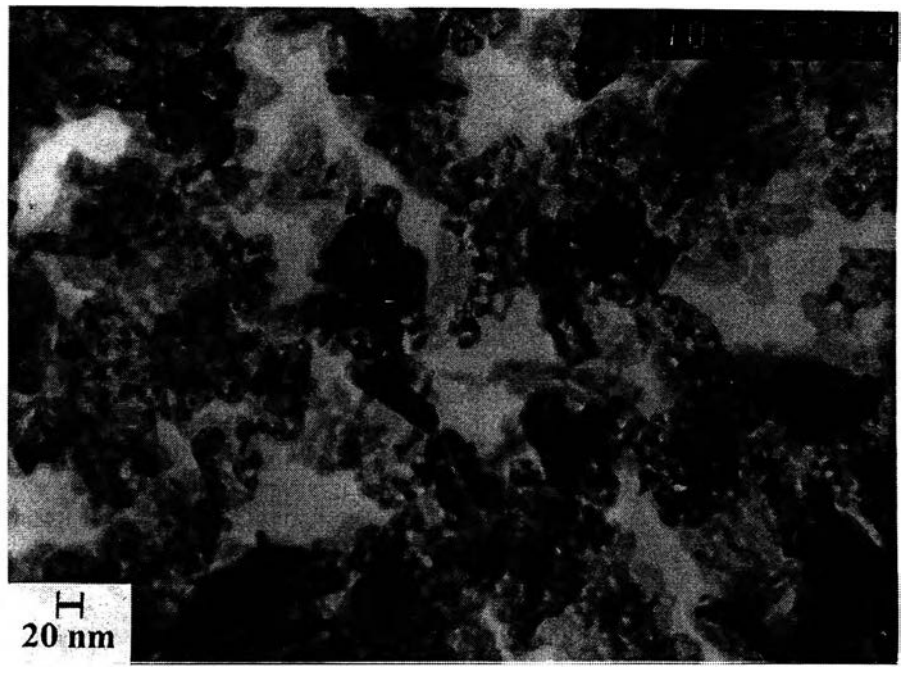

Figure 4.20 TEM micrograph of 0.12 wt.% Au/NiO calcined at 400°C

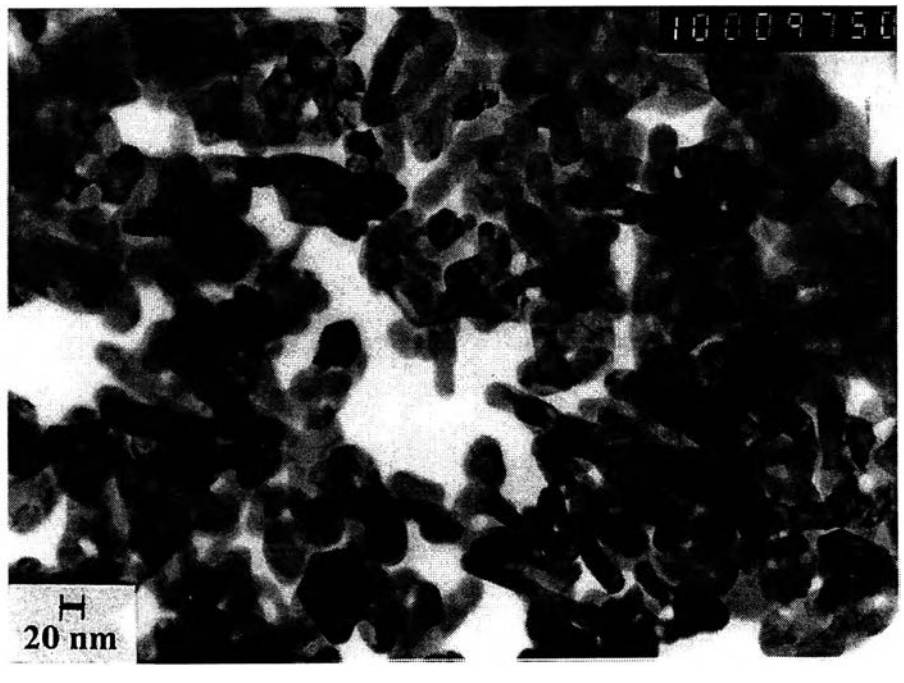

Figure 4.21 TEM micrograph of 0.12 wt.% Au/NiO calcined at 500°C

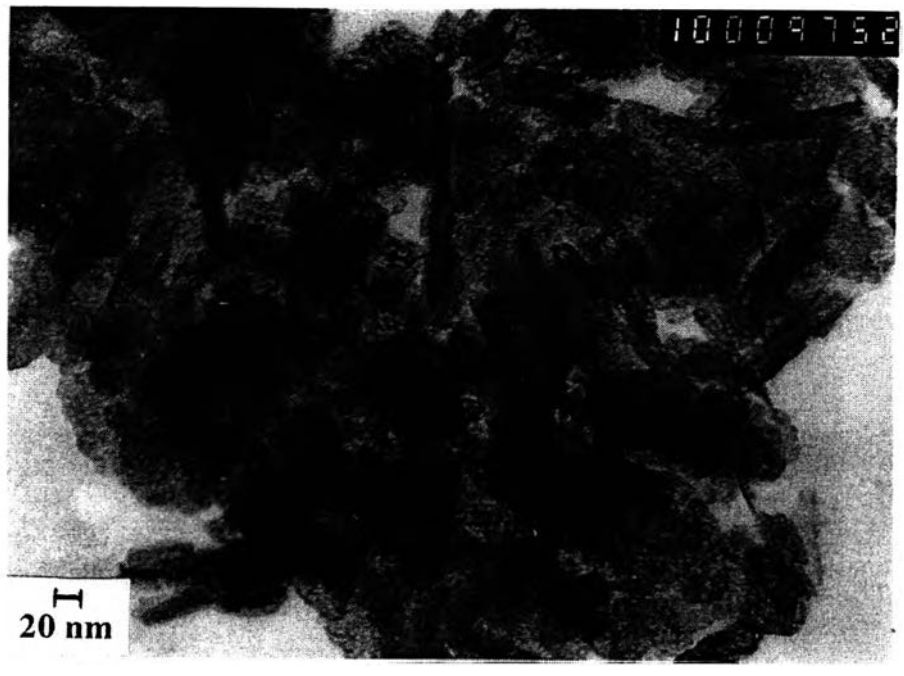

Figure 4.22 TEM micrograph of 0.22 wt.% Au/NiO calcined at 300°C

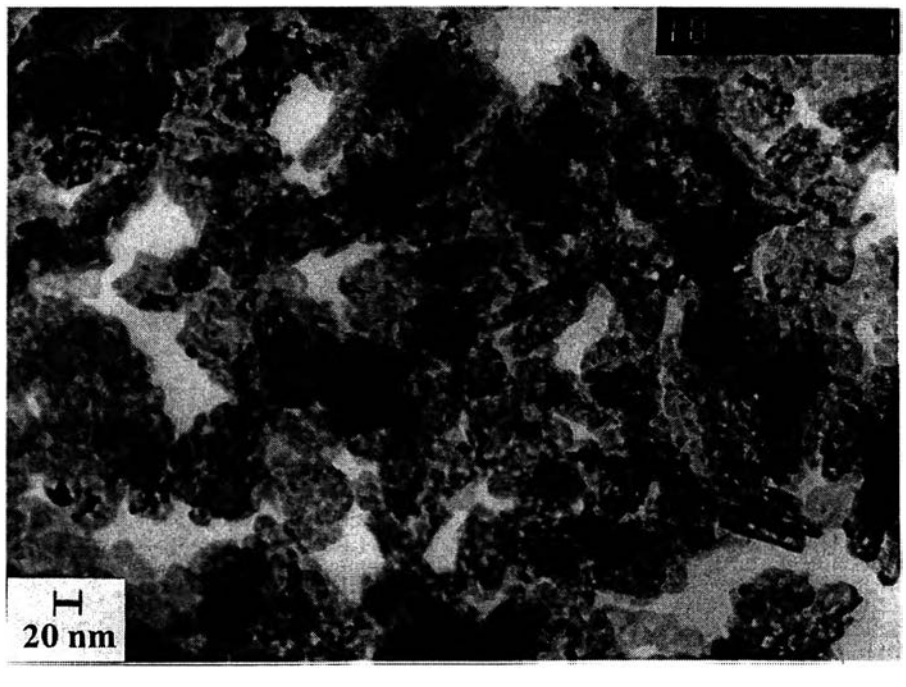

Figure 4.23 TEM micrograph of 0.22 wt.% Au/NiO calcined at 400°C

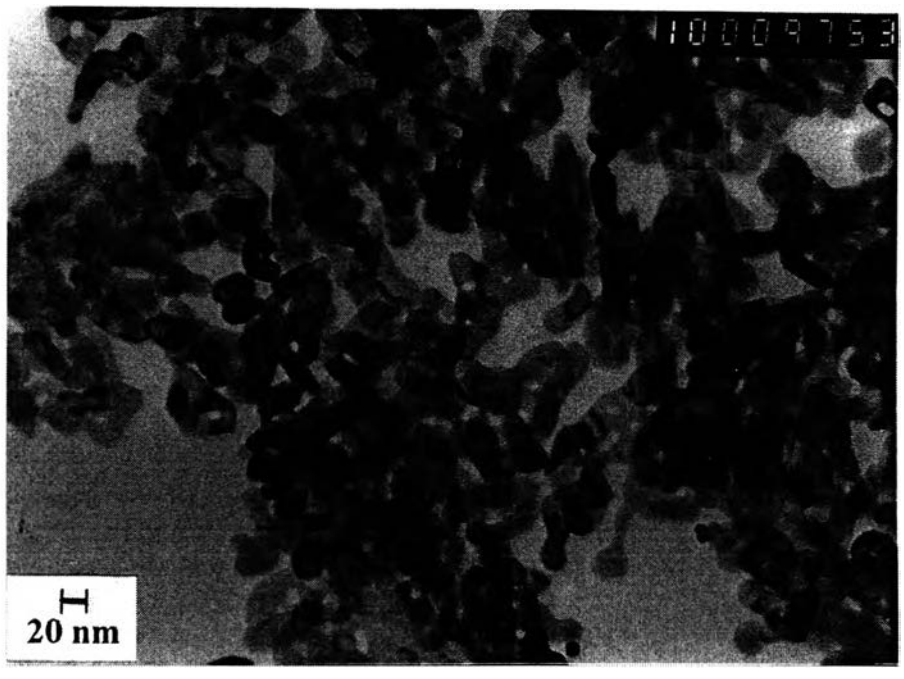

Figure 4.24 TEM micrograph of 0.22 wt.% Au/NiO calcined at 500°C

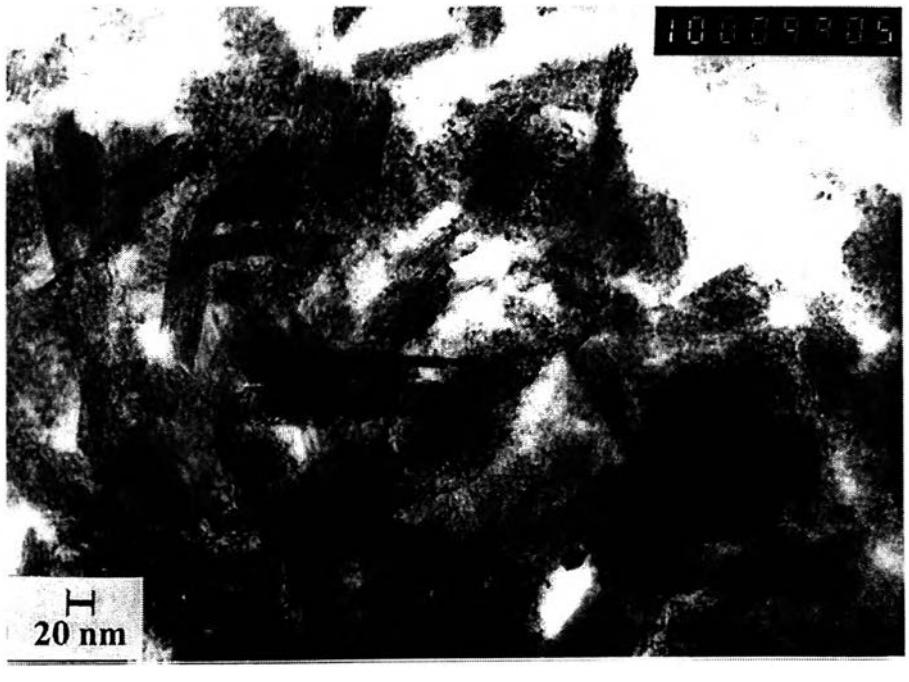

Figure 4.25 TEM micrograph of 1.74 wt.% Au/NiO calcined at 300°C

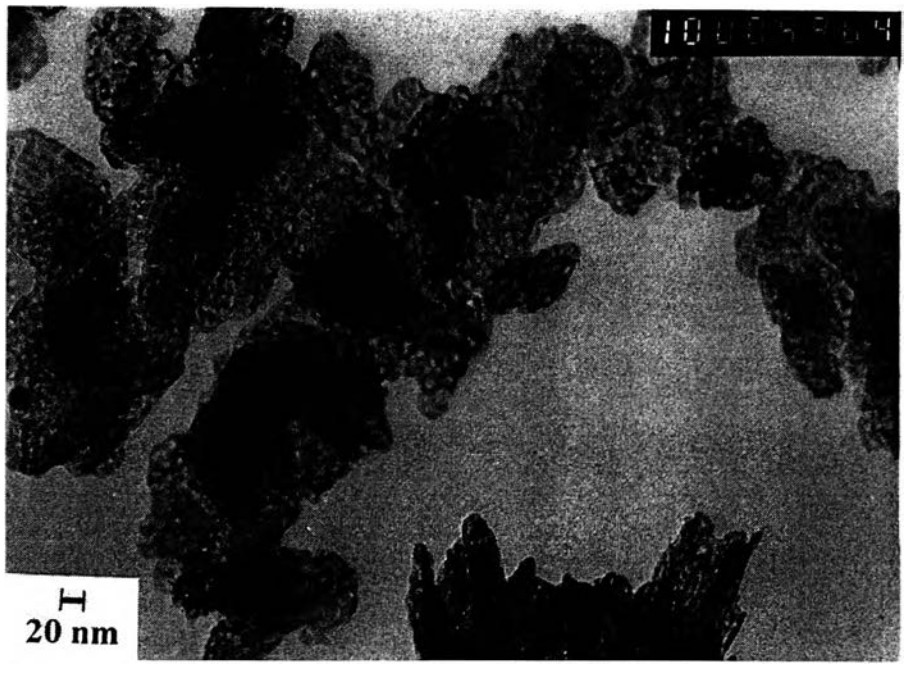

Figure 4.26 TEM micrograph of 1.74 wt.% Au/NiO calcined at 400°C

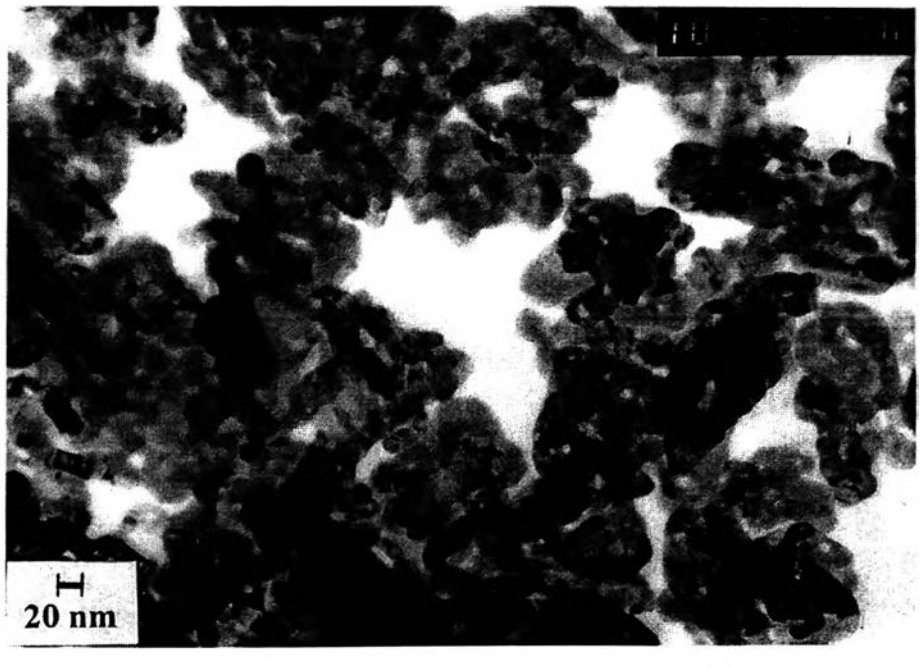

Figure 4.27 TEM micrograph of 1.74 wt.% Au/NiO calcined at 500°C

Figure 4.28 TEM micrograph of 0.48 wt.% Au/MnO_2 calcined at 300°C

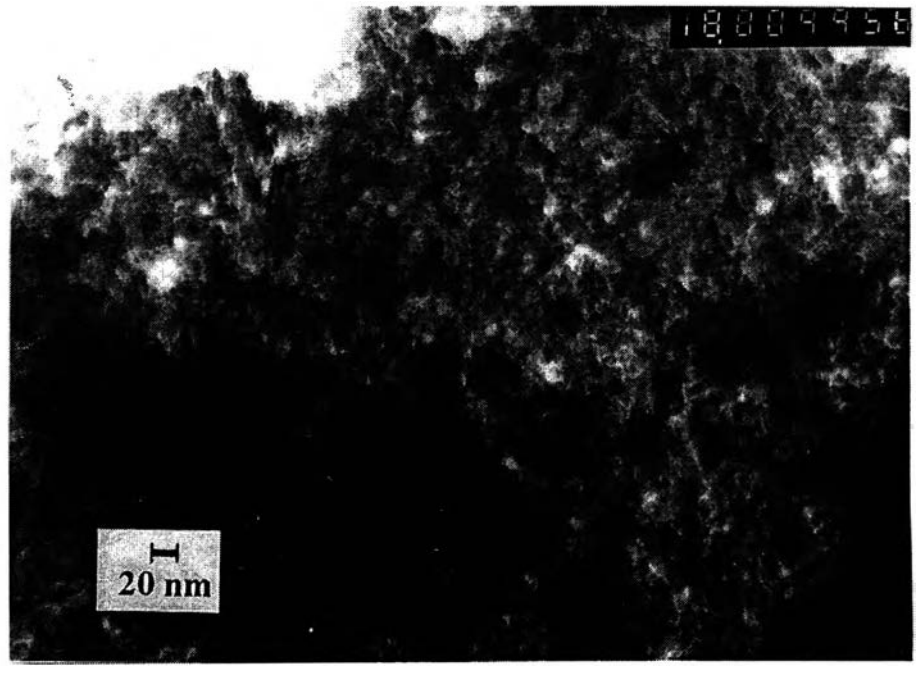

Figure 4.29 TEM micrograph of 0.48 wt.% Au/MnO_2 calcined at 400°C

I19359093

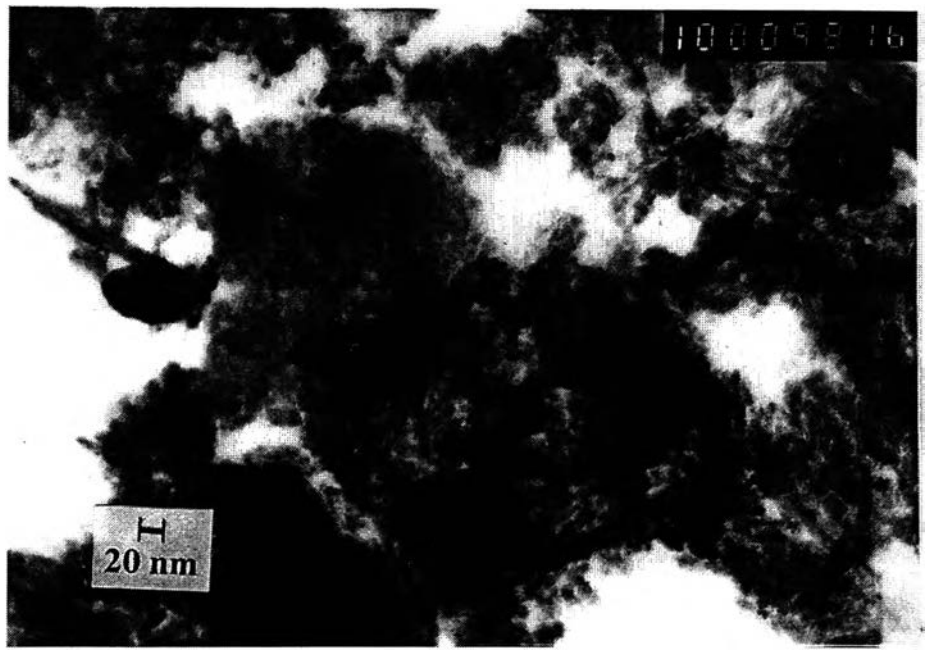

Figure 4.30 TEM micrograph of 0.48 wt.% Au/MnO_2 calcined at 500°C

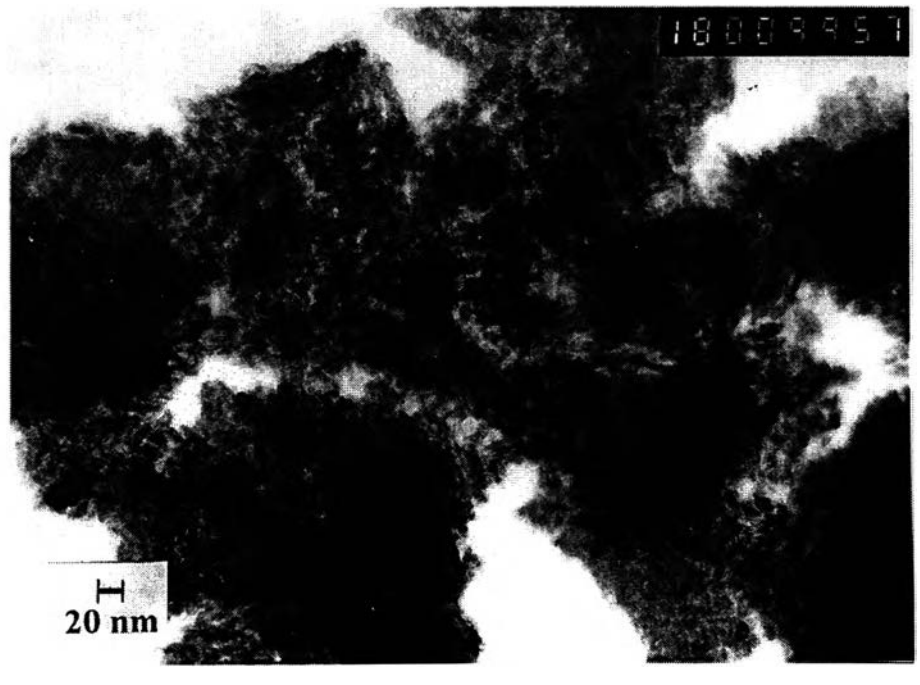

Figure 4.31 TEM micrograph of 0.95 wt.% Au/MnO_2 calcined at 300°C

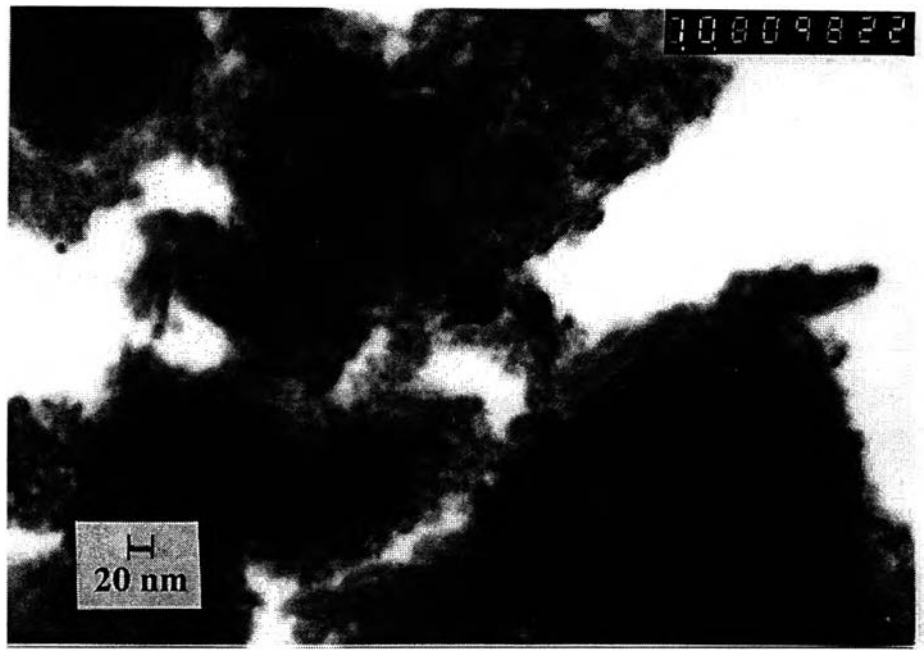

Figure 4.32 TEM micrograph of 0.95 wt.% Au/MnO_2 calcined at 400°C

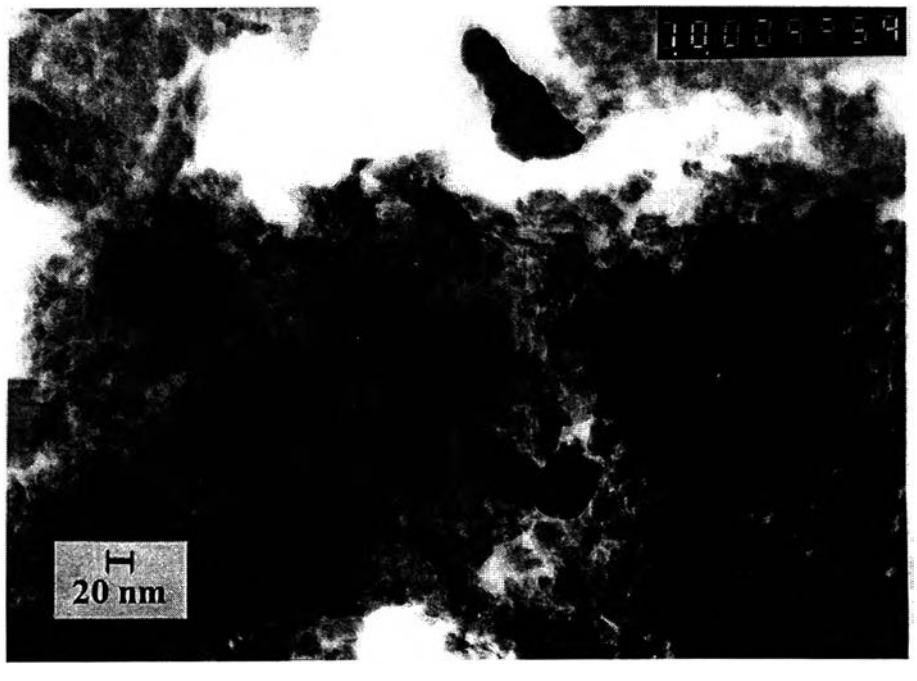

Figure 4.33 TEM micrograph of 0.95 wt.% Au/MnO_2 calcined at 500°C

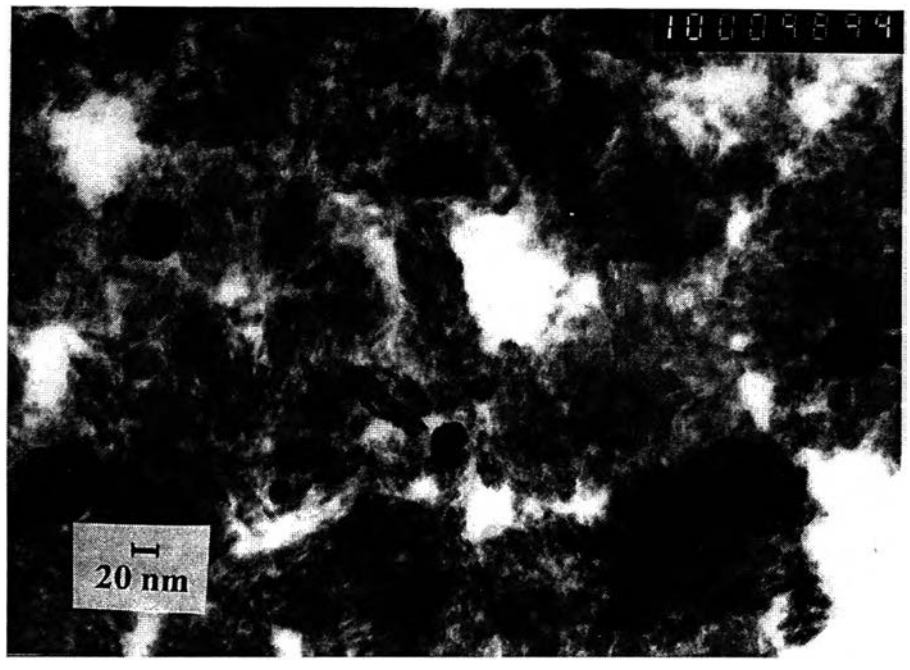

Figure 4.34 TEM micrograph of 1.40 wt.% Au/MnO_2 calcined at 300°C

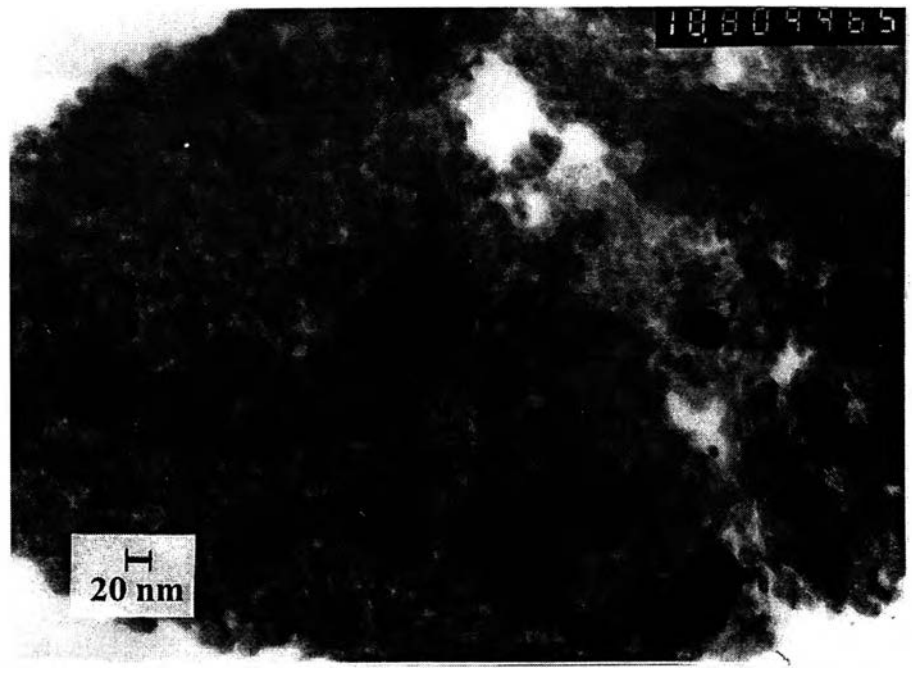

Figure 4.35 TEM micrograph of 1.40 wt.% Au/MnO_2 calcined at 400°C

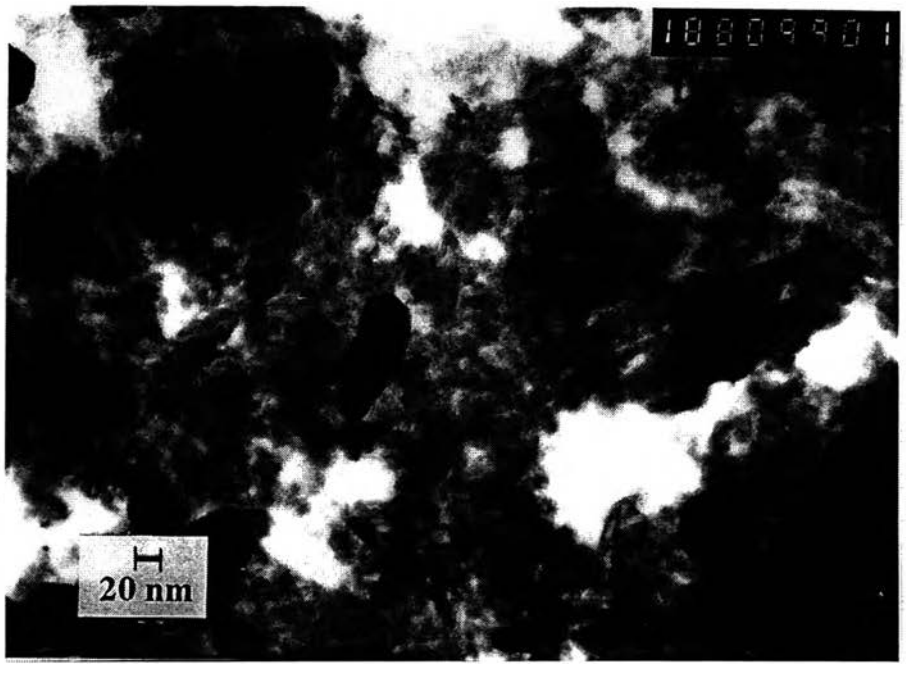

Figure 4.36 TEM micrograph of 1.40 wt.% Au/MnO_2 calcined at 500°C

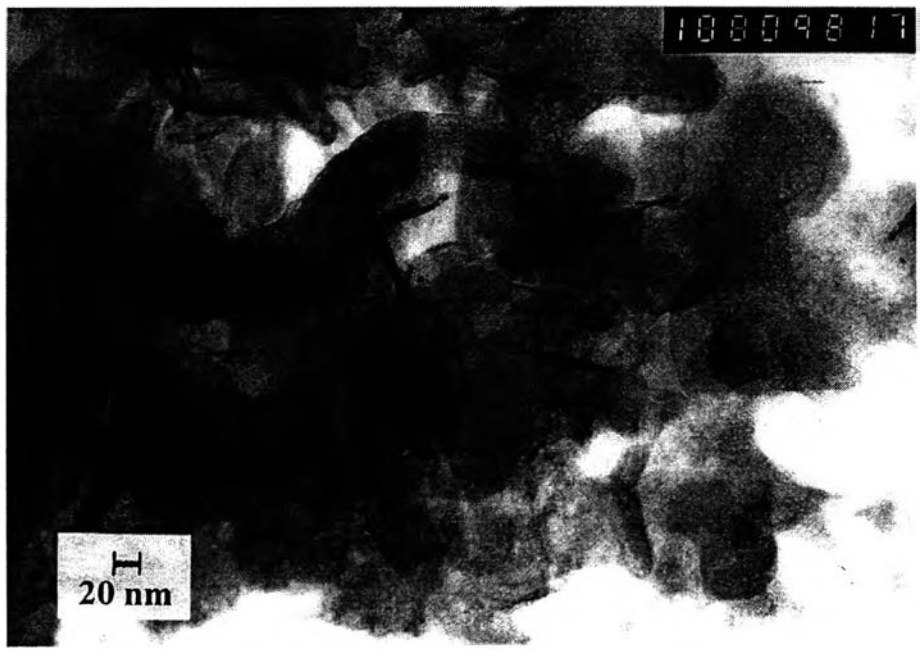

Figure 4.37 TEM micrograph of 0.18 wt.% Au/Y_2O_3 calcined at 300°C

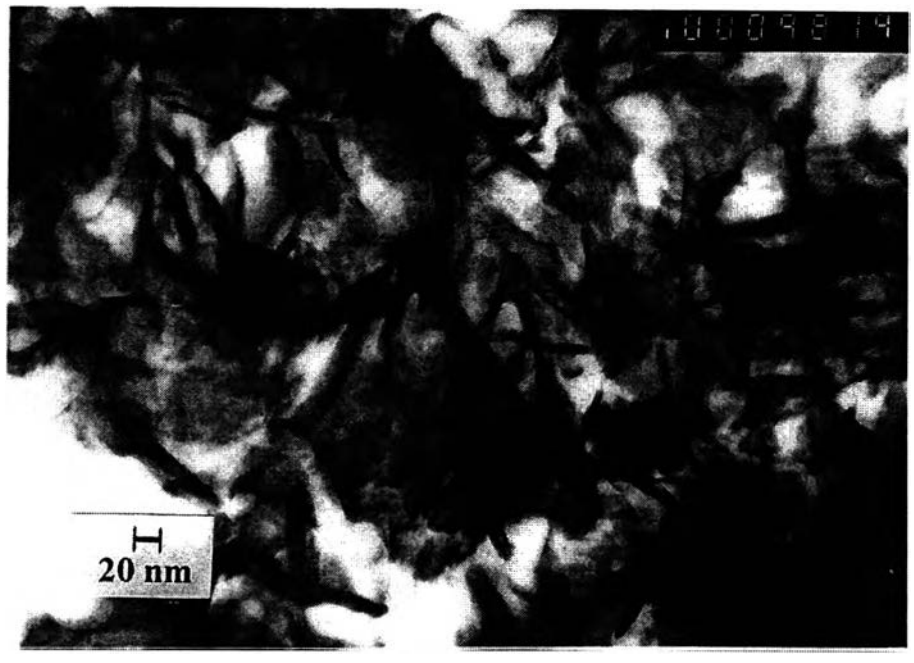

Figure 4.38 TEM micrograph of 0.18 wt.% Au/Y_2O_3 calcined at 400°C

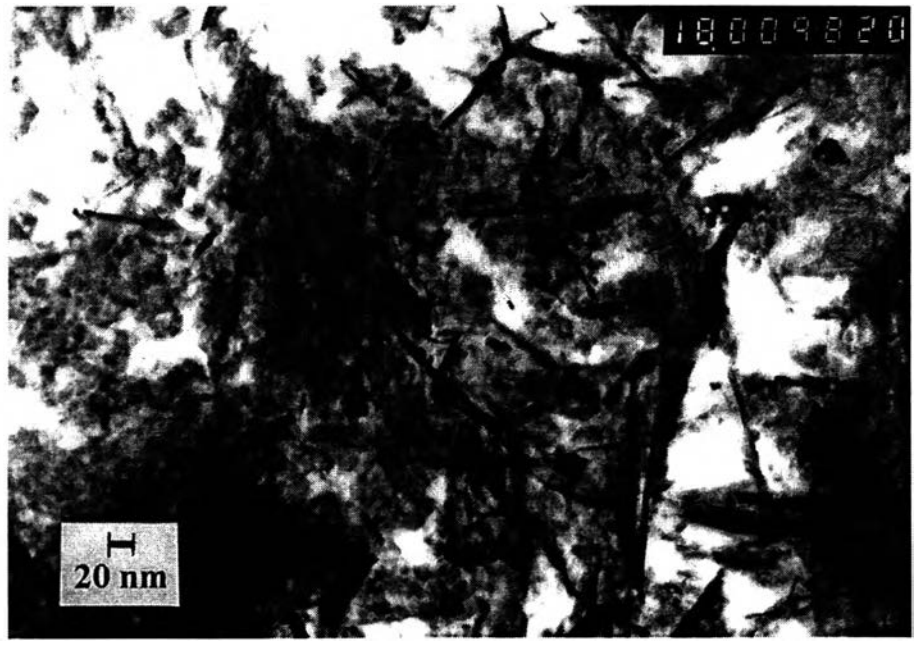

Figure 4.39 TEM micrograph of 0.18 wt.% Au/Y_2O_3 calcined at 500°C

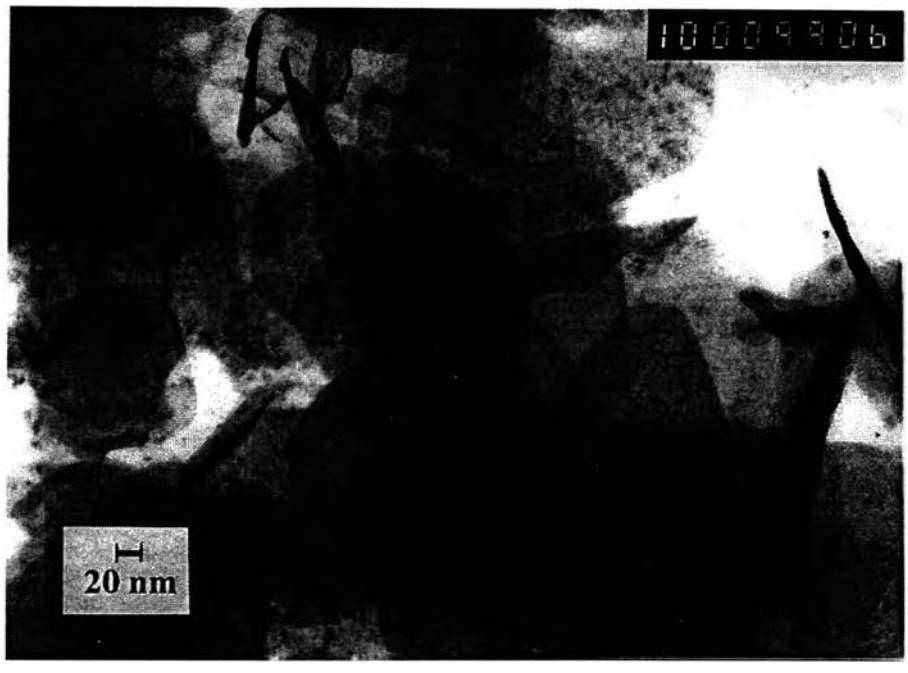

Figure 4.40 TEM micrograph of 0.23 wt.% Au/Y_2O_3 calcined at 300°C

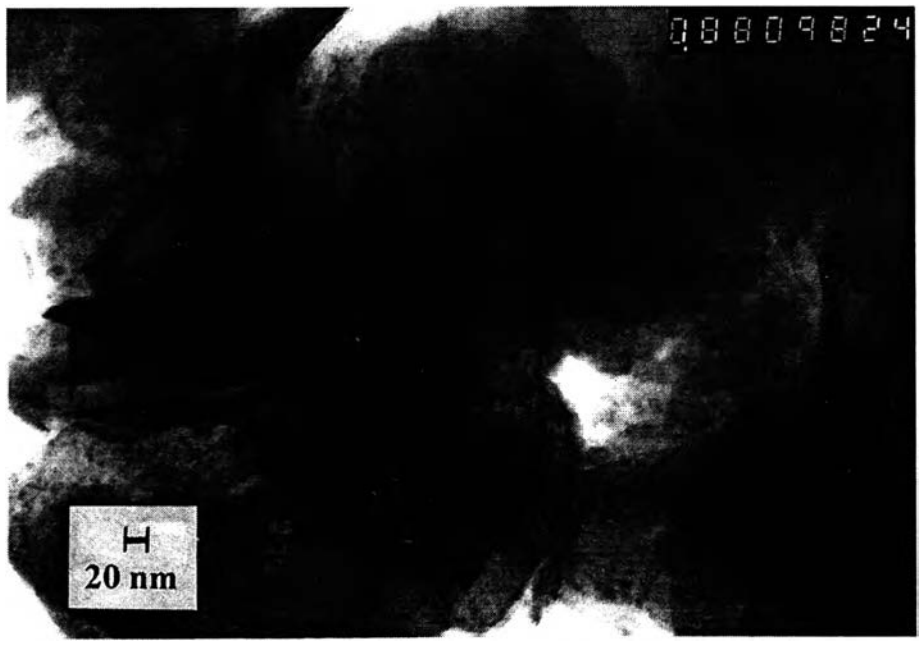

Figure 4.41 TEM micrograph of 0.23 wt.% Au/Y_2O_3 calcined at 400°C

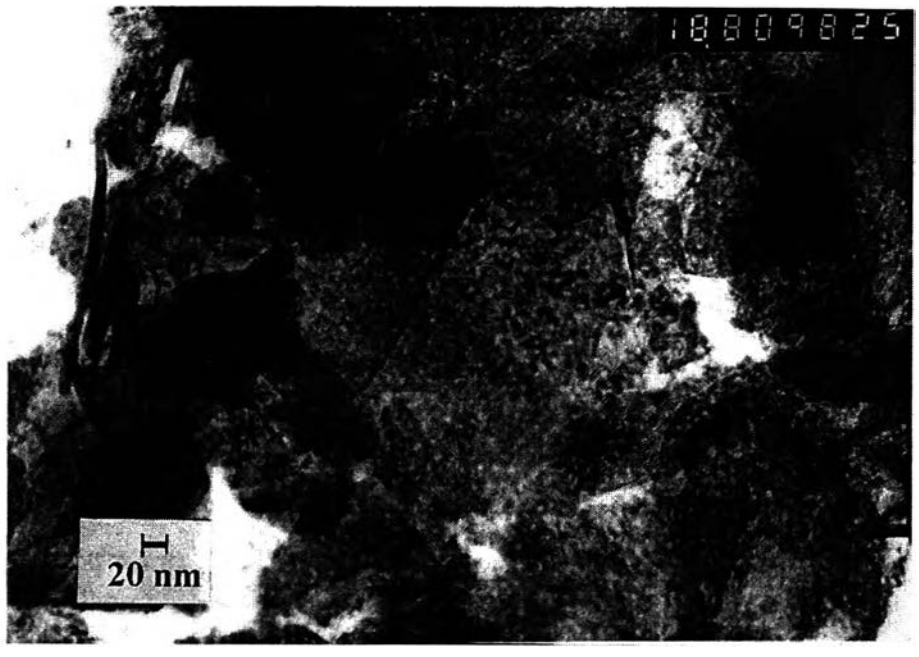

Figure 4.42 TEM micrograph of 0.23 wt.% Au/Y_2O_3 calcined at 500°C

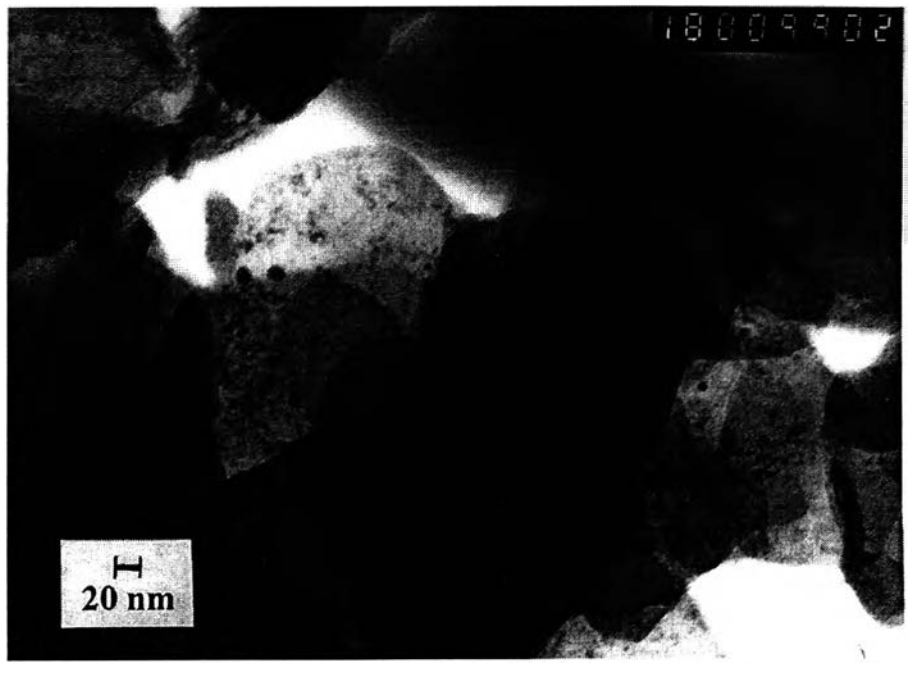

Figure 4.43 TEM micrograph of 0.58 wt.% Au/Y_2O_3 calcined at 300°C

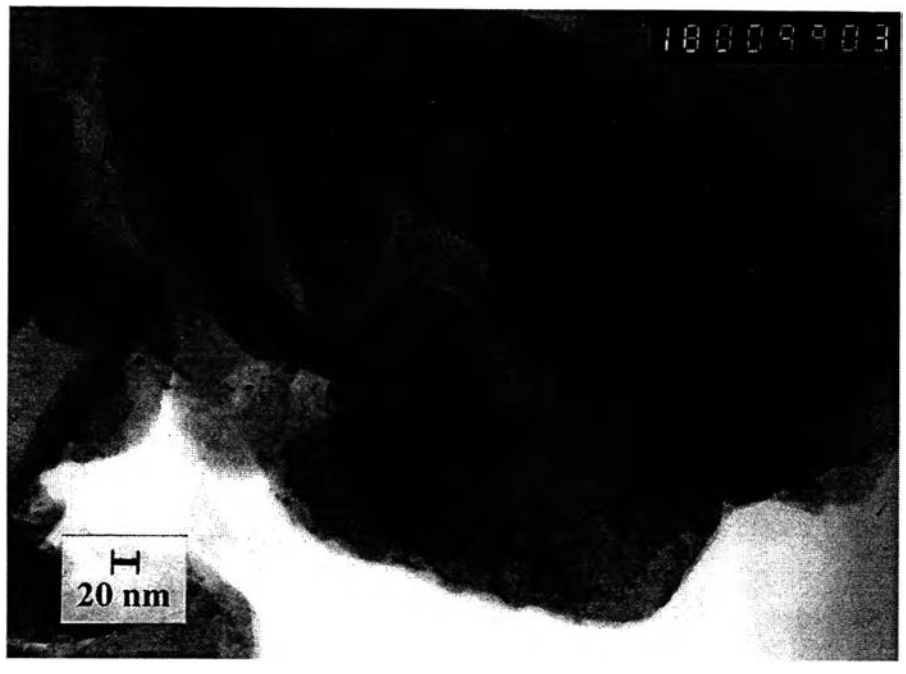

Figure 4.44 TEM micrograph of 0.58 wt.% Au/Y_2O_3 calcined at 400°C

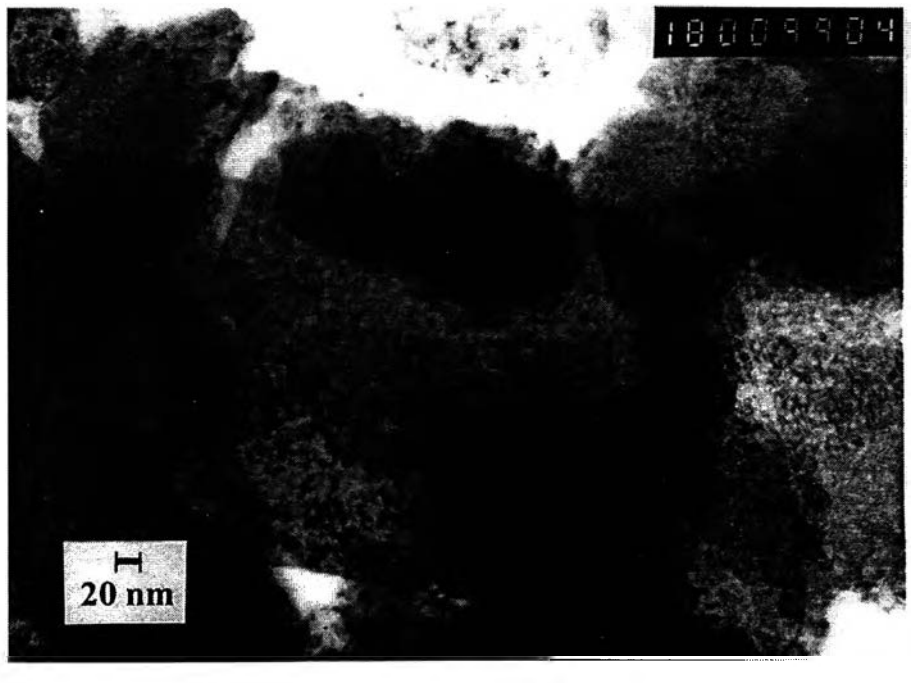

Figure 4.45 TEM micrograph of 0.58 wt.% Au/Y_2O_3 calcined at 500°C

micrographs reveal that a higher calcination temperature gave a higher gold particle size for Au/NiO catalysts. The gold particles sizes on NiO support were about less than 5 nm, between 5 and 10 nm, and larger than 10 nm when the catalysts were calcined at 300°C, 400°C, and 500°C, respectively. Interestingly, the morphologies of NiO calcined at 300°C (Figures 4.19, 4.22, and 4.25) are different from those calcined at 400°C (Figures 4.20, 4.23, and 4.26) and 500°C (Figures 4.21, 4.24, and 4.27). In addition, the morphology of NiO calcined at 300°C was less crystallite than those calcined at 400°C and 500°C. This result also agrees with the XRD patterns of NiO as described earlier.

For Au/MnO_2, Changing in morphology of MnO_2 was almost not obvious. However, at least, calcination temperature should affect the morphology of MnO_2 because BET surface area, as shown in previous section, decreased with increasing calcination temperature. This change may be transformation from one type to another type, eg. α or β or γ or δ form, but it stills to be the same specie (MnO_2).

For Au/Y_2O_3, morphology of catalysts calcined at 300°C and 400°C looked similar but they were obviously different from that calcined at 500°C. The morphology of Au/Y_2O_3 calcined at 300°C and 400°C are amorphous whereas crystalline structure of Au/Y_2O_3 was found at calcination temperature of 500°C. This result agrees with the XRD results because the XRD patterns of catalysts calcined at 300°C and 400°C are similar but obviously different from that calcined at 500°C.

4.6 Temperature-programmed Desorption

The temperature-programmed desorption (TPD) of oxygen for all catalysts with different gold contents supported on NiO, MnO_2 and Y_2O_3 were carried

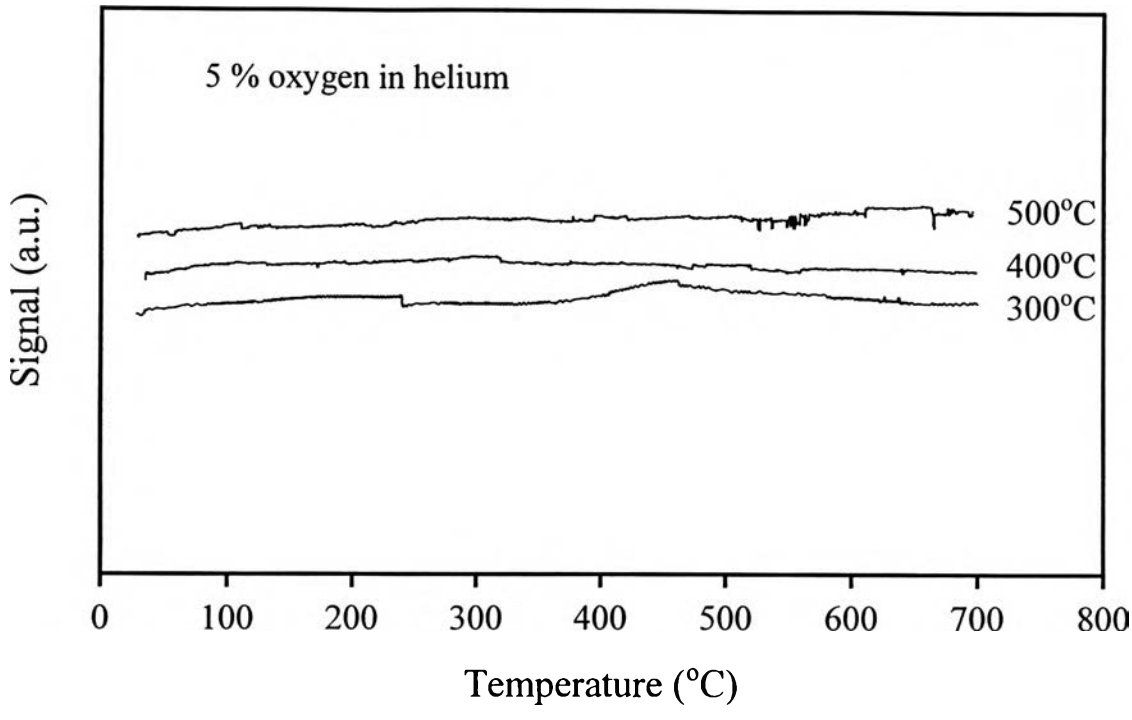

Figure 4.46 Temperature-programmed desorption of oxygen for 0.12 wt.% Au/NiO calcined at different temperatures

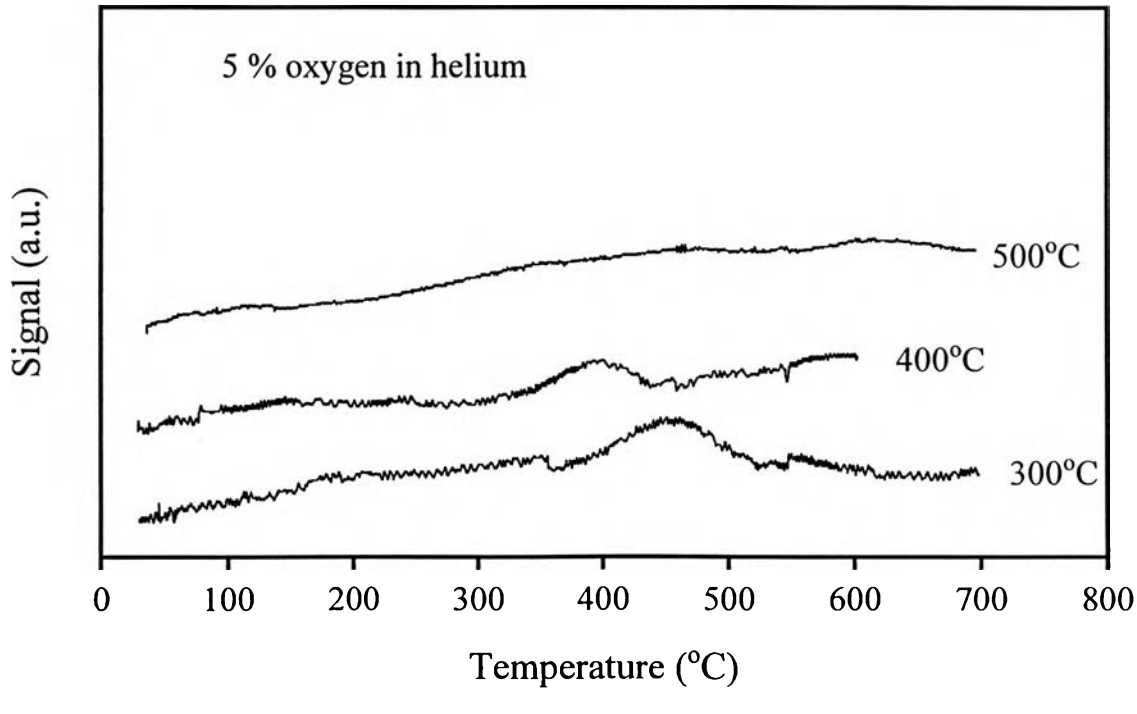

Figure 4.47 Temperature-programmed desorption of oxygen for 0.22 wt.% Au/NiO calcined at different temperatures

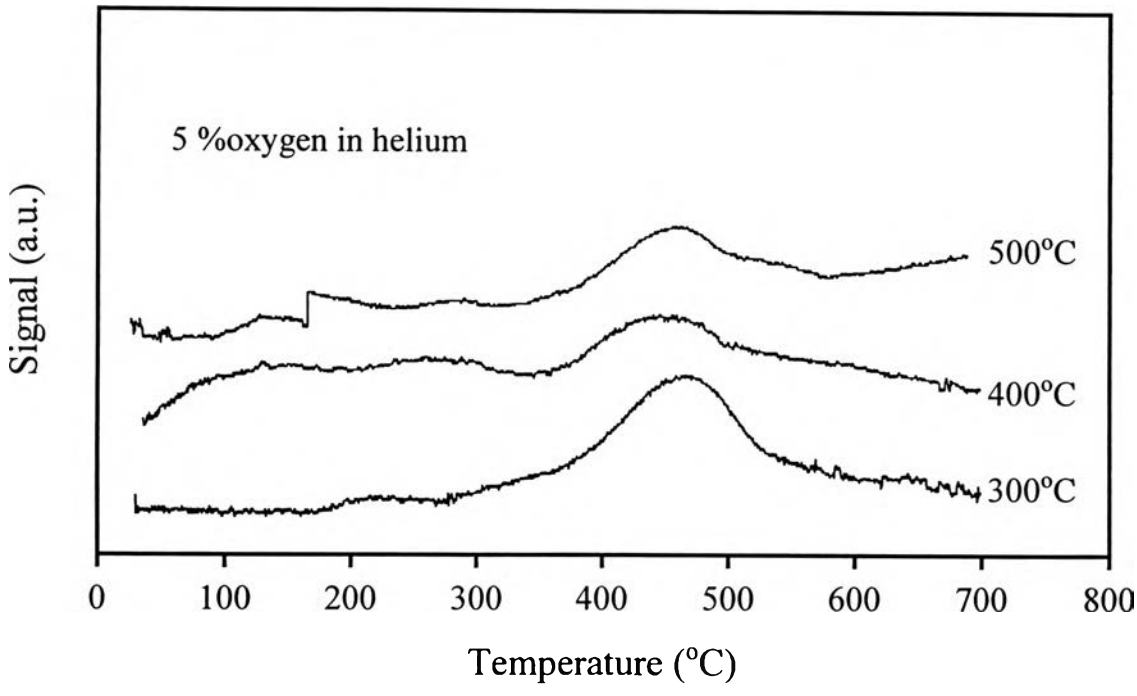

Figure 4.48 Temperature-programmed desorption of oxygen for 1.74 wt.% Au/NiO calcined at different temperatures

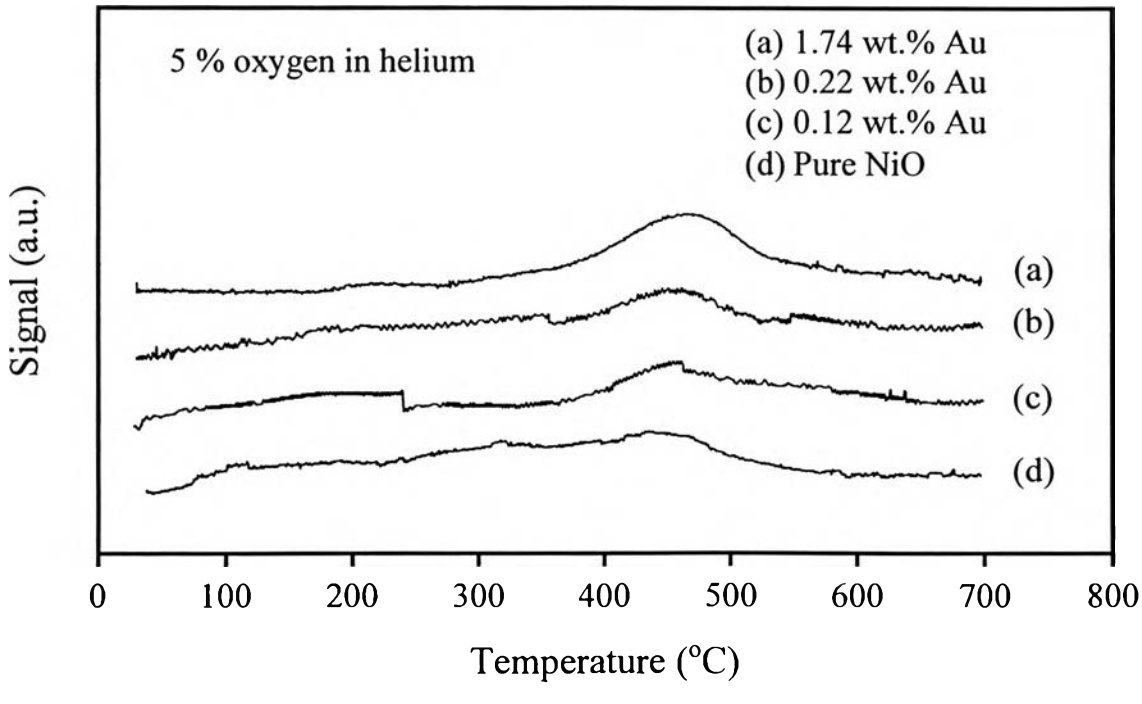

Figure 4.49 Temperature-programmed desorption of oxygen for a series of Au/NiO catalysts calcined at 300°C

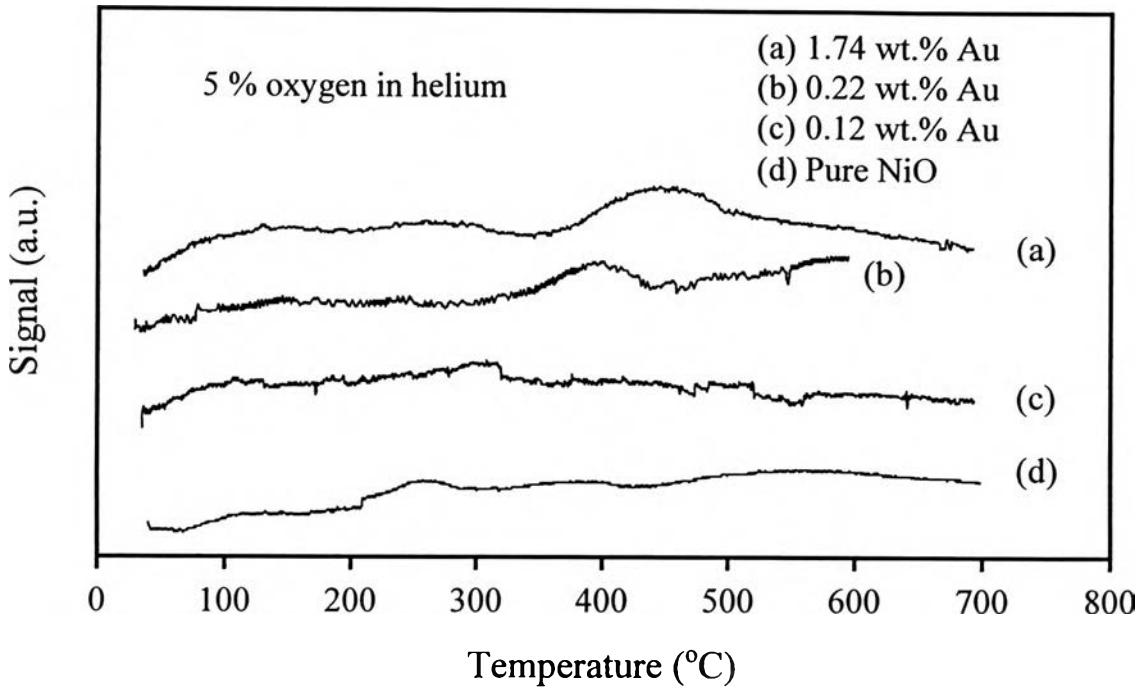

Figure 4.50 Temperature-programmed desorption of oxygen for a series of Au/NiO catalysts calcined at 400°C

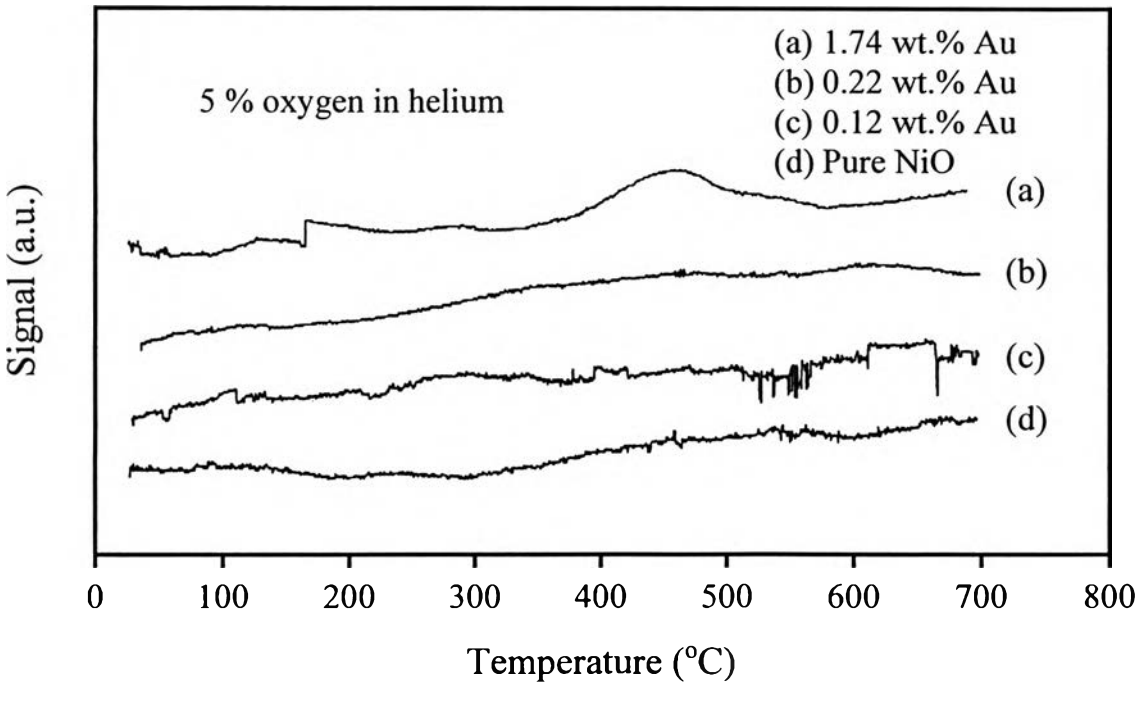

Figure 4.51 Temperature-programmed desorption of oxygen for a series of Au/NiO catalysts calcined at 500°C

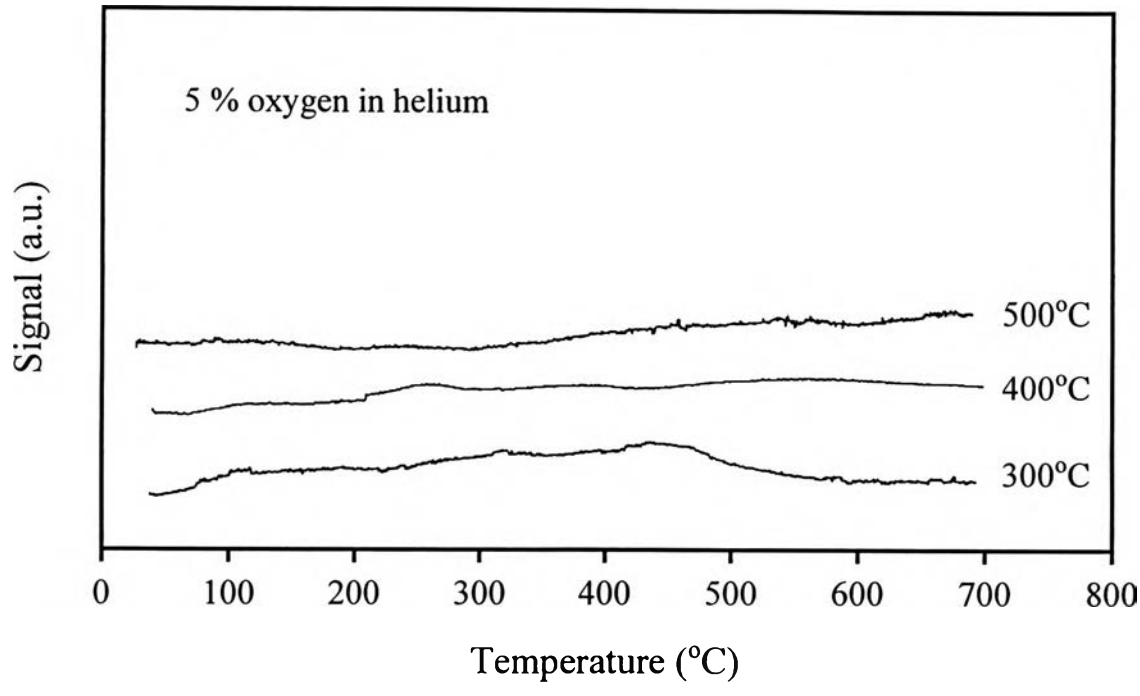

Figure 4.52 Temperature-programmed desorption of oxygen for pure NiO calcined at different temperatures

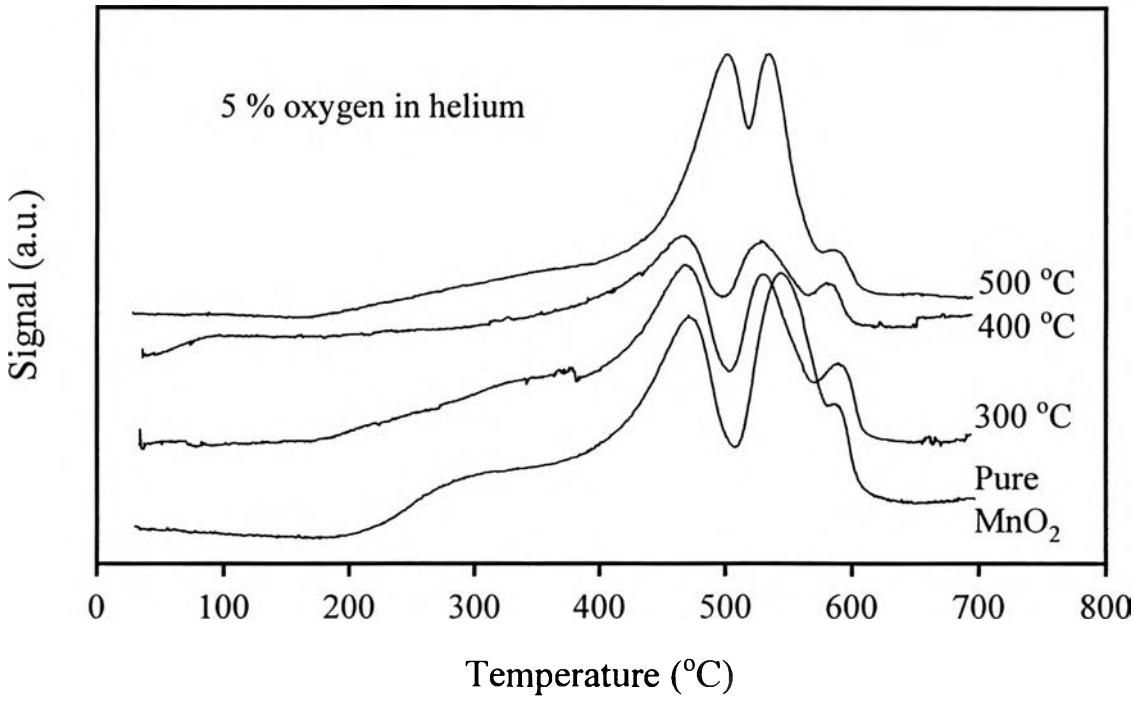

Figure 4.53 Temperature-programmed desorption of oxygen for 0.48 wt.% Au/MnO_2 and MnO_2 powder calcined at different temperatures

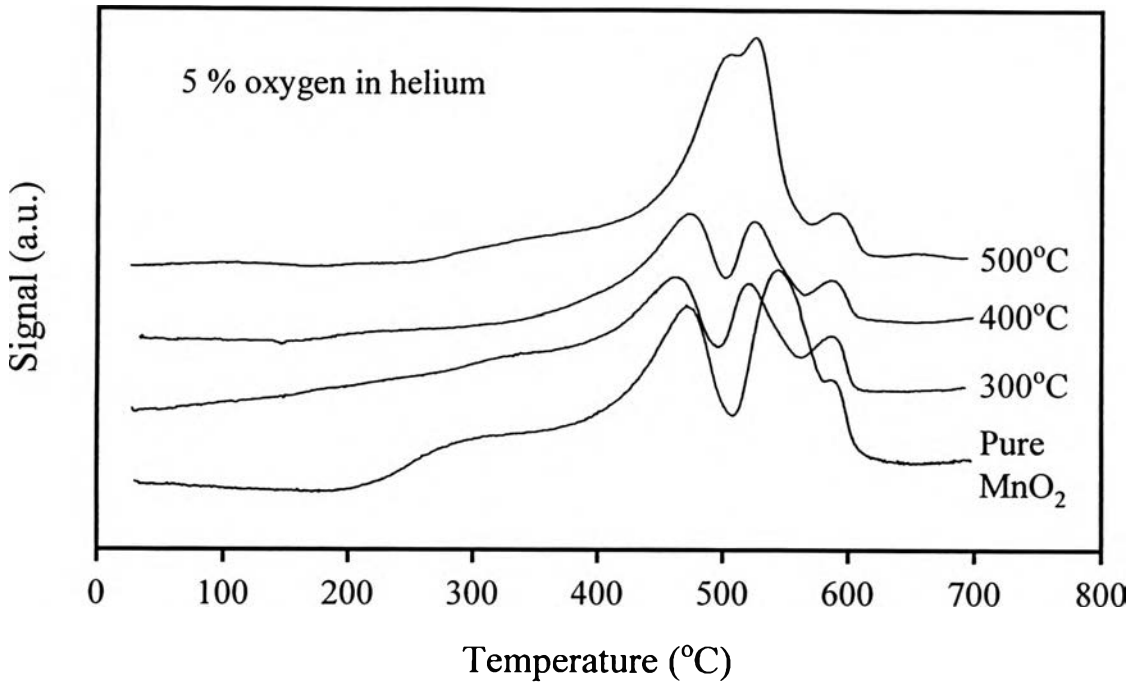

Figure 4.54 Temperature-programmed desorption of oxygen for 0.95 wt.% Au/MnO_2 and MnO_2 powder calcined at different temperatures

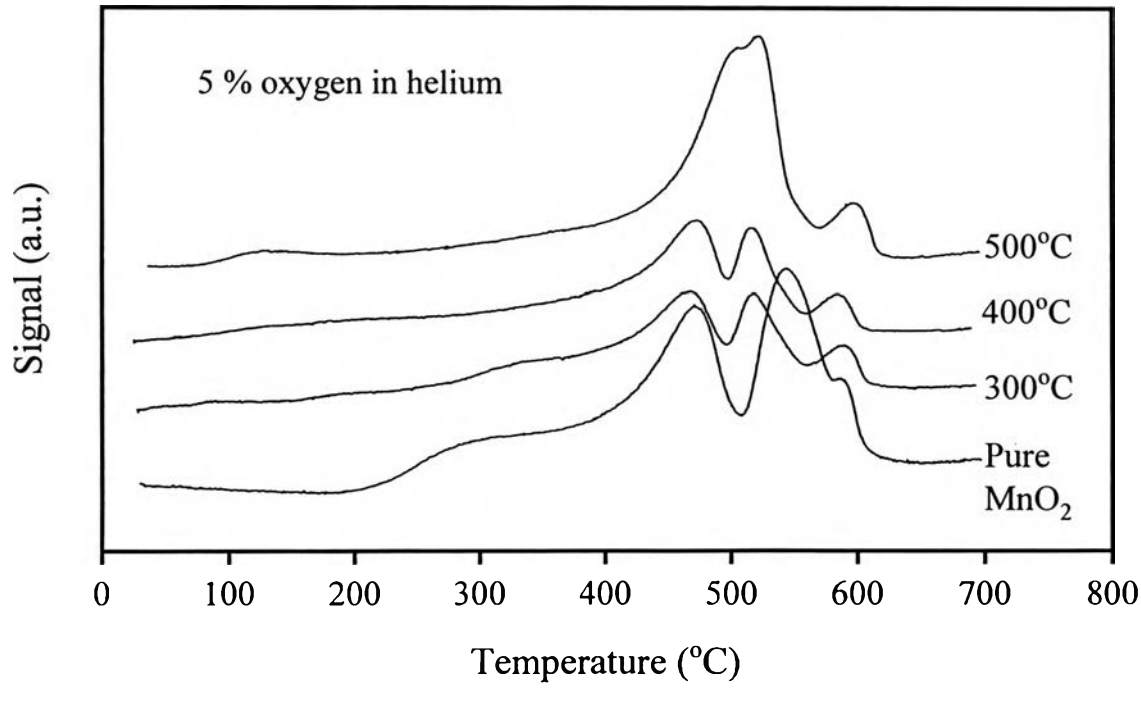

Figure 4.55 Temperature-programmed desorption of oxygen for 1.40 wt.% Au/MnO_2 and MnO_2 powder calcined at different temperatures

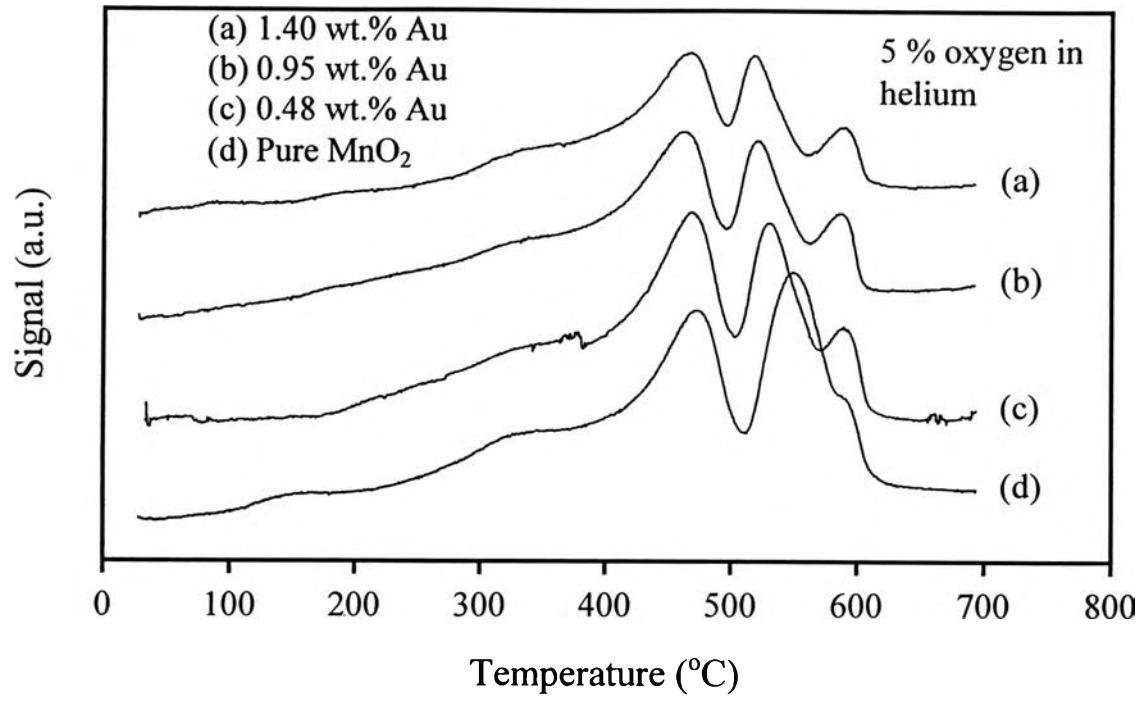

Figure 4.56 Temperature-programmed desorption of oxygen for a series of Au/MnO_2 and MnO_2 powder calcined at 300°C

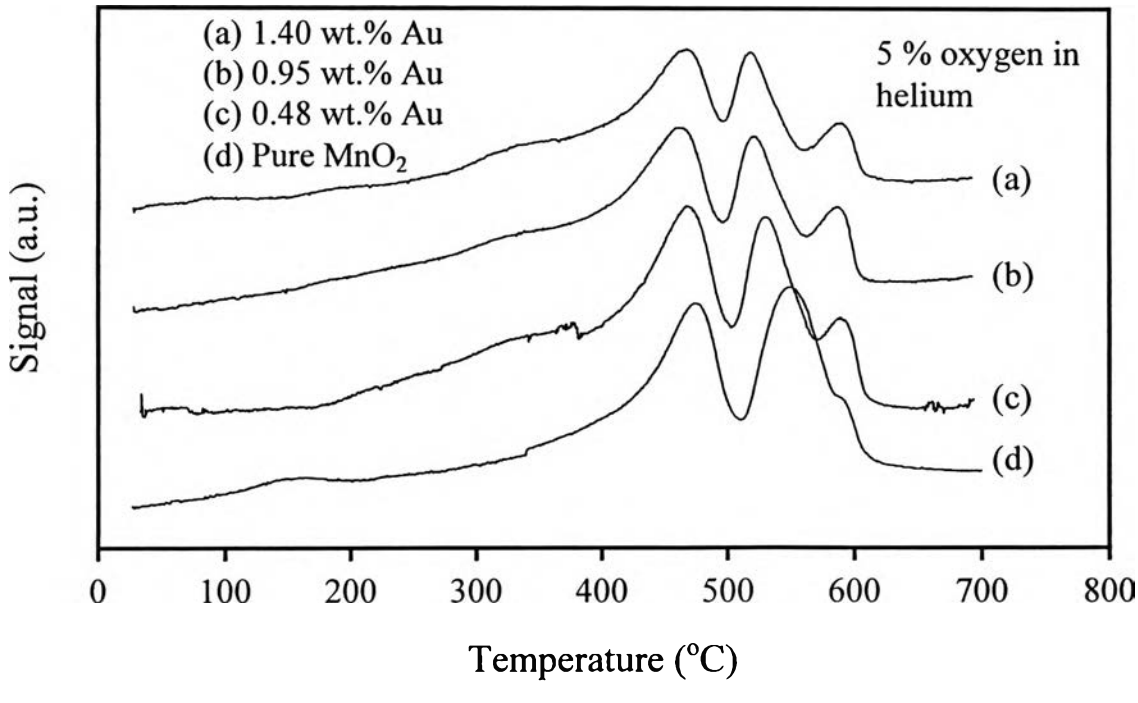

Figure 4.57 Temperature-programmed desorption of oxygen for a series of Au/MnO_2 and MnO_2 powder calcined at 400°C

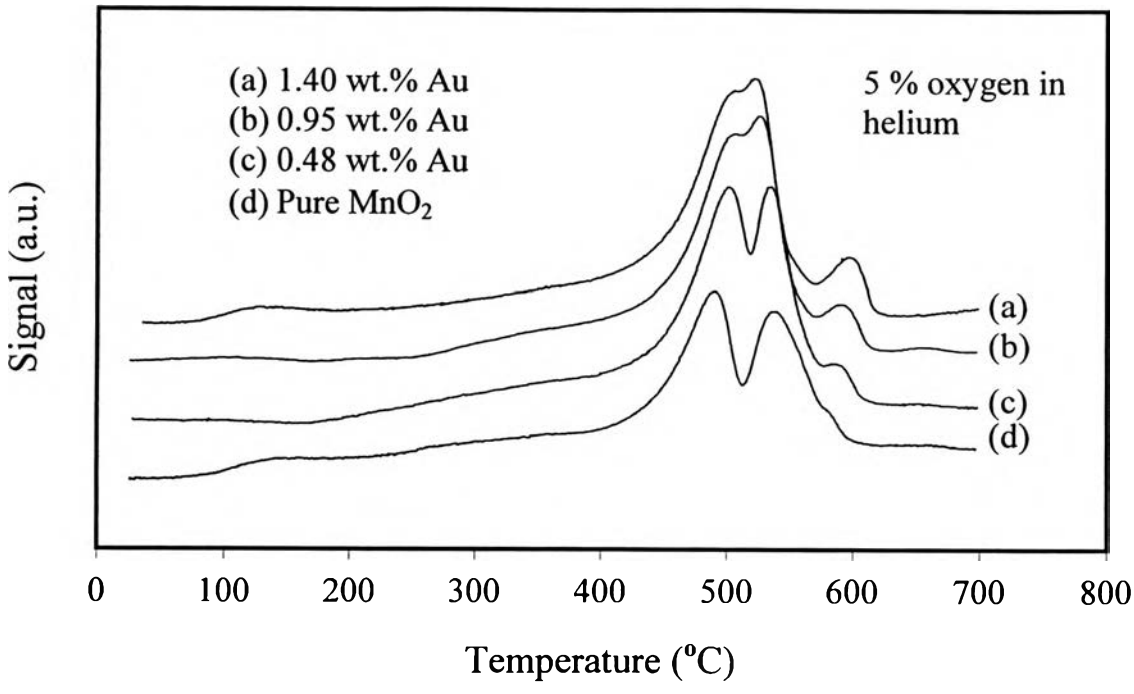

Figure 4.58 Temperature-programmed desorption of oxygen for a series of Au/MnO_2 and MnO_2 powder calcined at 500°C

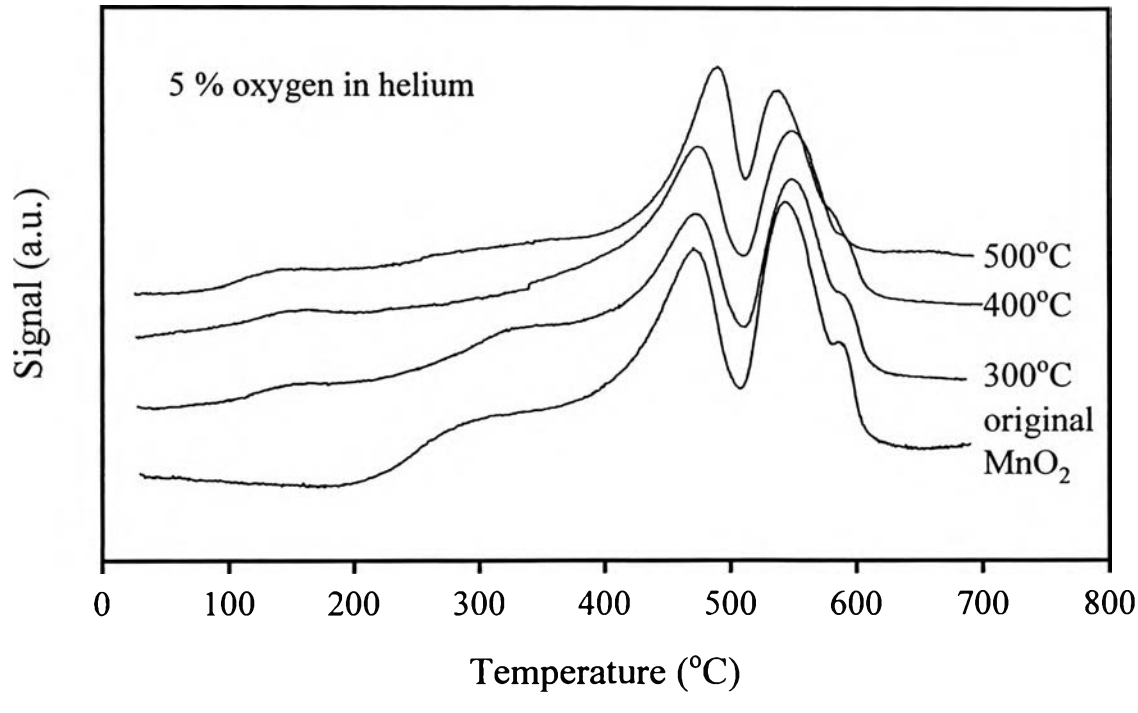

Figure 4.59 Temperature-programmed desorption of oxygen for MnO_2 calcined at different temperatures

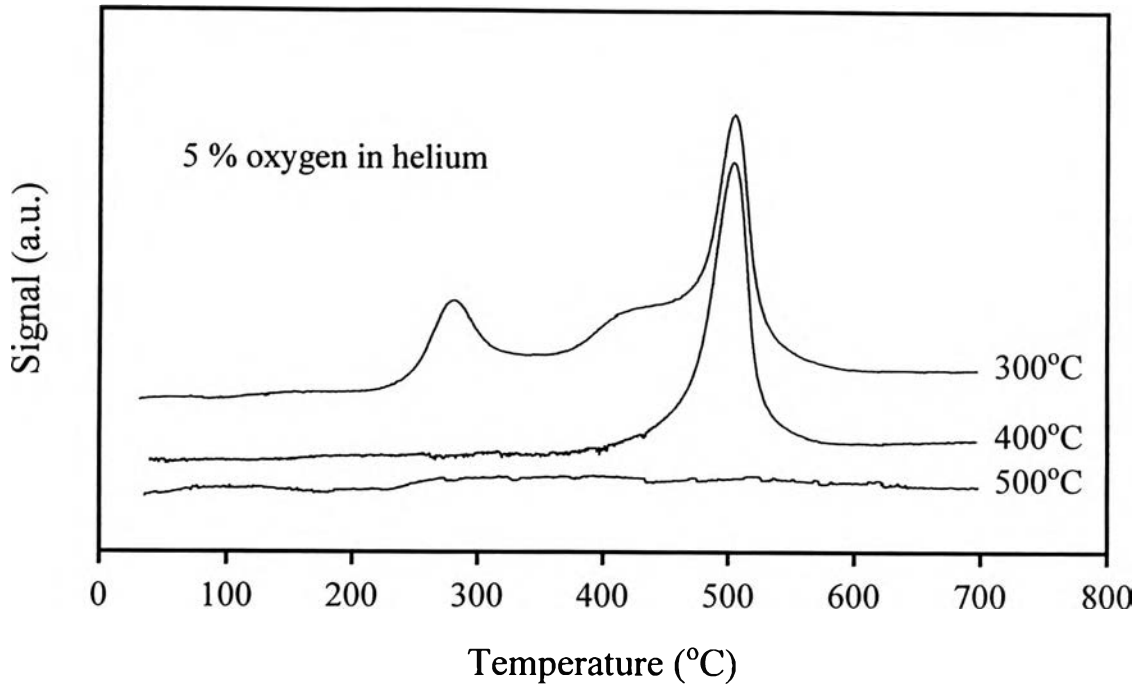

Figure 4.60 Temperature-programmed desorption of oxygen for 0.18 wt.% Au/Y_2O_3 calcined at different temperatures

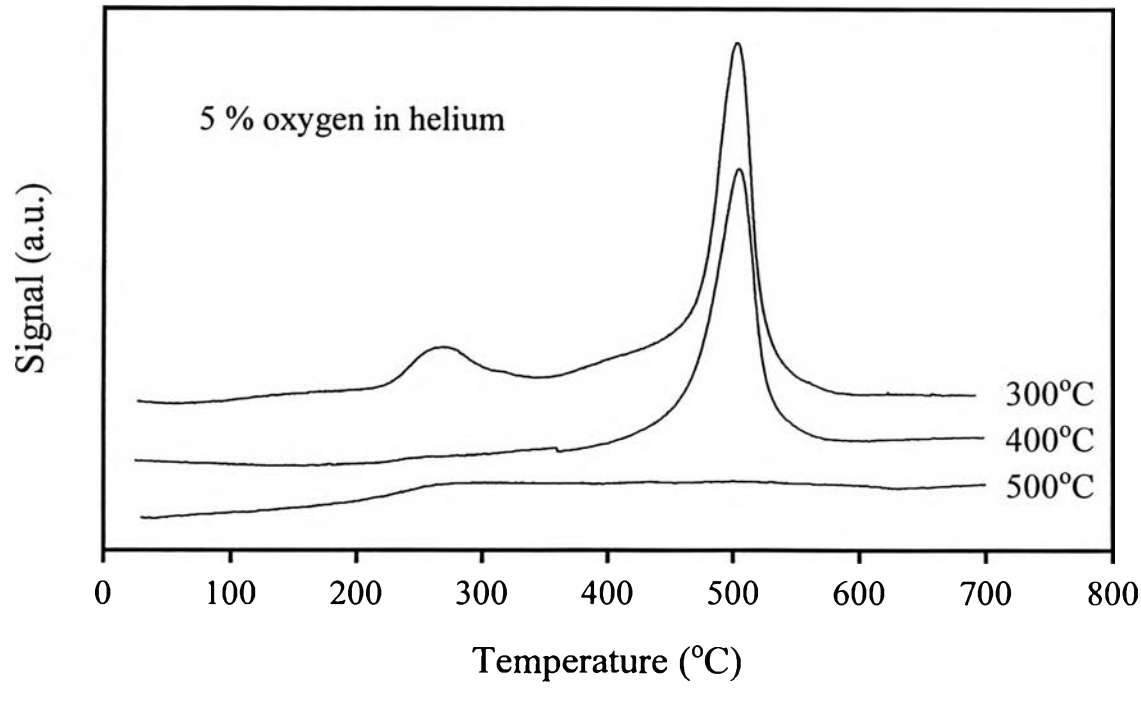

Figure 4.61 Temperature-programmed desorption of oxygen for 0.23 wt.% Au/Y_2O_3 calcined at different temperatures

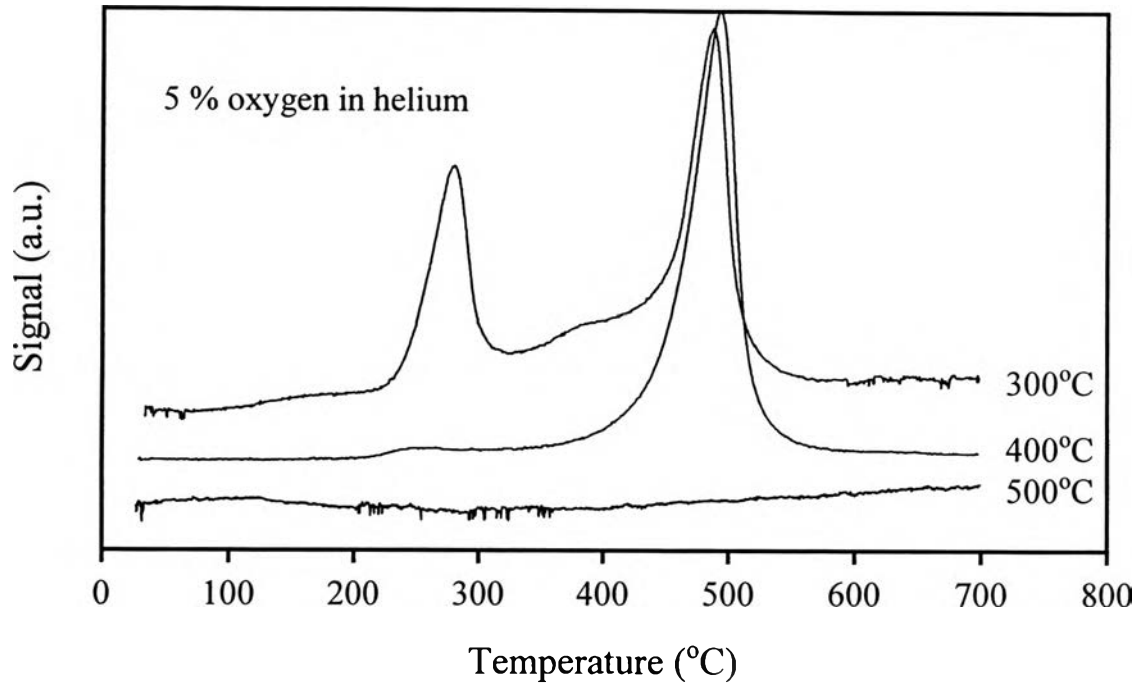

Figure 4.62 Temperature-programmed desorption of oxygen for 0.58 wt.% Au/Y_2O_3 calcined at different temperatures

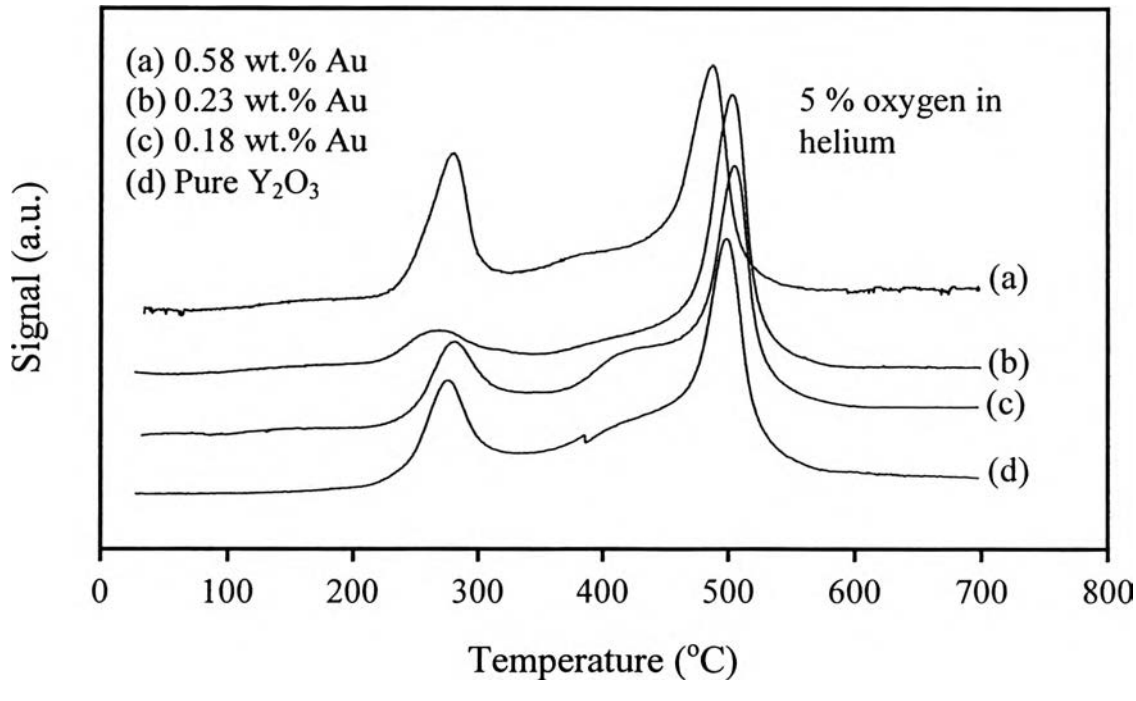

Figure 4.63 Temperature-programmed desorption of oxygen for a series of Au/Y_2O_3 calcined at 300°C

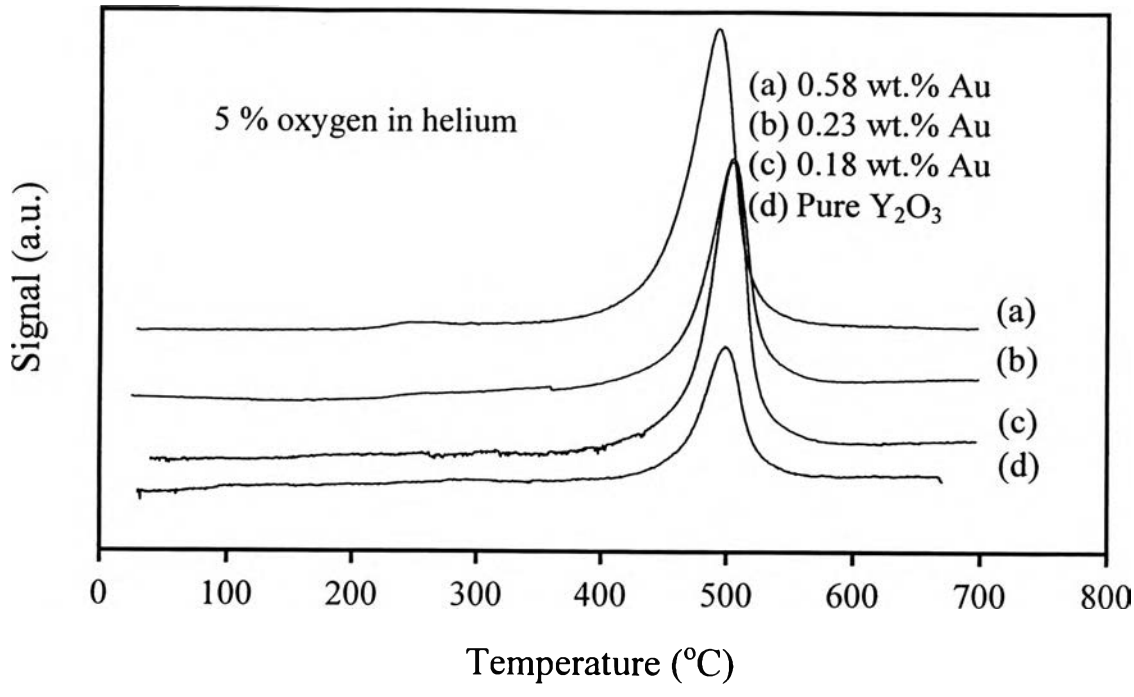

Figure 4.64 Temperature-programmed desorption of oxygen for a series of Au/Y_2O_3 calcined at 400°C

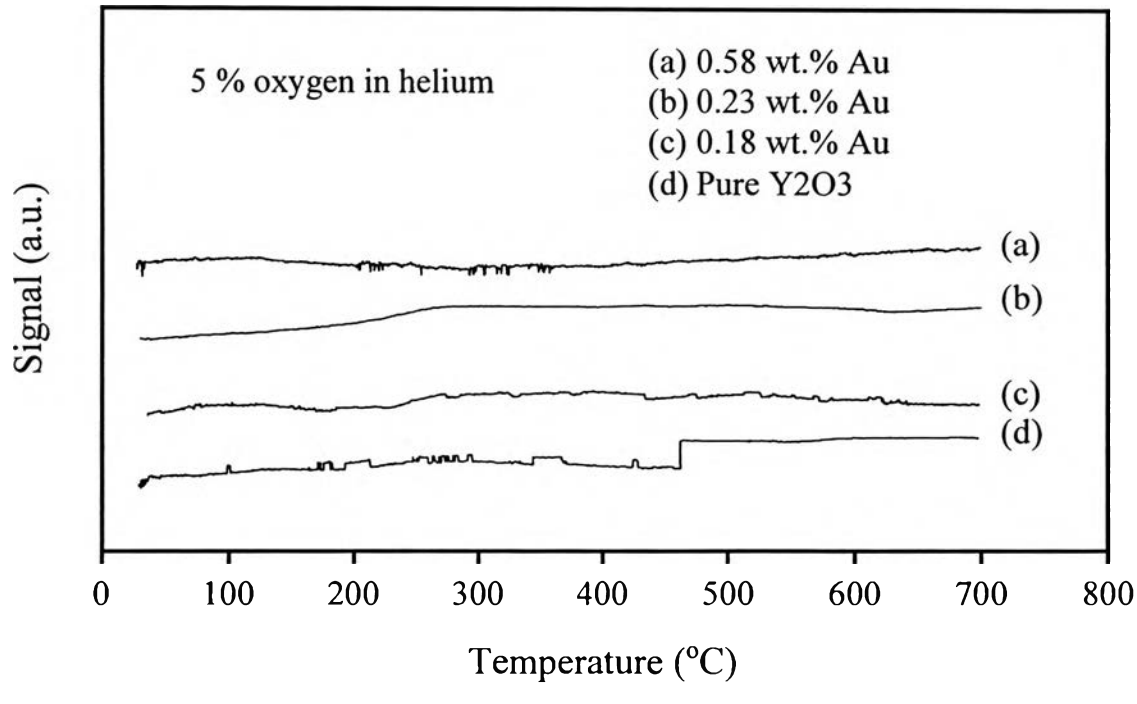

Figure 4.65 Temperature-programmed desorption of oxygen for a series of Au/Y_2O_3 calcined at 500°C

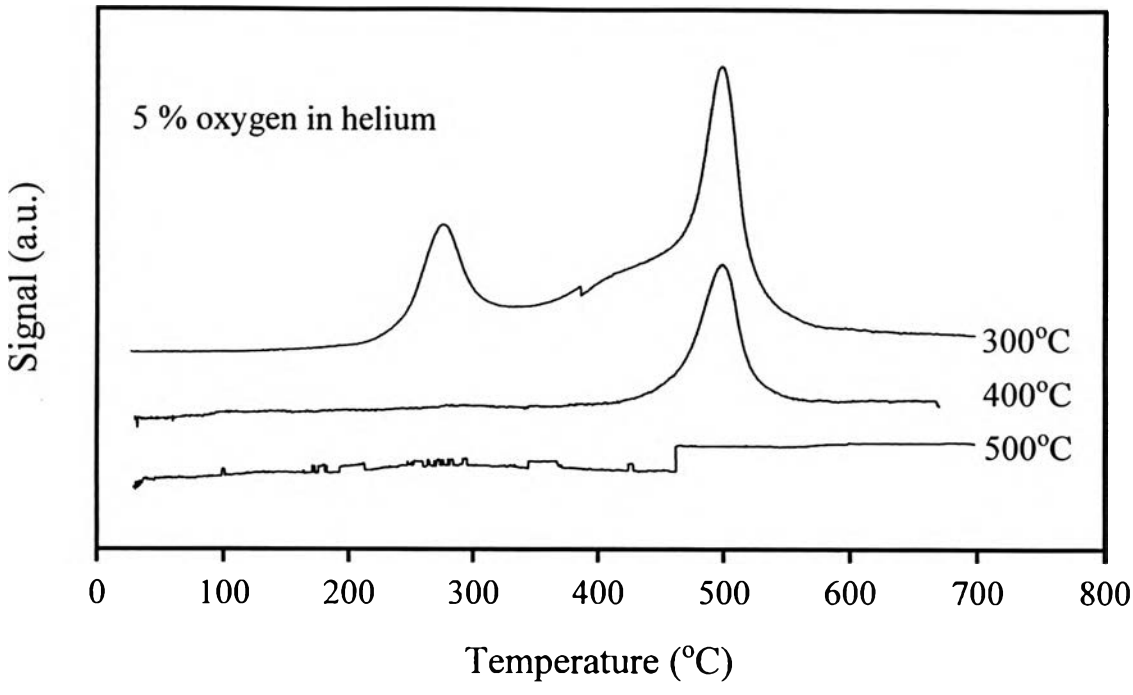

Figure 4.66 Temperature-programmed desorption of oxygen for pure Y_2O_3 calcined at different temperatures

out with 5 % oxygen in helium at room temperature. Figures 4.46-4.66 show the TPD profiles of oxygen for all catalysts prepared. Figures 4.46-4.48 show the TPD profiles of 0.12 wt.%, 0.22 wt.%, and 1.74 wt.% of gold catalysts supported on NiO calcined at different temperatures. It can be seen clearly that there was a very tiny broad peak at about 450°C for the catalyst calcined at temperature of 300°C for doping level of 0.12 wt.%. For the doping level of 0.22 wt.%, there were two desorption peaks appearing at 450°C and 400°C when calcination temperatures were 300°C and 400°C, respectively. For the highest doping level (1.74 wt.%), the desorption temperature for the catalyst calcined at 400°C appeared at the lowest temperature of 430°C. In addition, the desorption peak for calcination temperature of 500°C could be observed when the gold loading was at the highest value of 1.74 wt.%. For showing the effect of gold loading, on the TPD profiles, for any given calcination temperature, the TPD profiles are reploted at various gold loadings as shown

in Figures 4.49-4.51. For a calcinatiom temperature of 300°C (Figure 4.49), it can be seen clearly that desorption temperatures for all doping levels are almost the same. Interestingly, at calcination temperature of 400°C (Figure 4.50), the lowest desorption temperature of 400°C is obtained when the doping level is 0.22 wt.%. However, for a calcinatiom temperature of 500°C (Figure 4.51), no desorption peak occur except for the highest doping level of 1.74 wt.%. Figure 4.52 shows that there is no any peak appearing when pure NiO calcined at different temperatures are tested. Based on the results, it can be concluded that gold supported on NiO could enhance adsorption and desorption properties of oxygen. The optimum calcination tempreature for the lowest desorption temperature was 400°C and the optimum gold loading was 0.22 wt.% for Au/NiO catalysts.

Figures 4.53, 4.54 and 4.55 show the TPD profiles of 5 % oxygen for MnO_2 powder without calcination compared to those for a series of Au/MnO_2 catalysts loading 0.48 wt.%, 0.95 wt.%, and 1.40 wt.% and calcined at different temperatures. Figures 4.56-4.58 show the TPD profiles of oxygen for pure MnO_2 compared to those for various amount of gold loaded on MnO_2 at calcination temperature of 300°C, 400°C, and 500°C. Figure 4.59 shows the TPD profiles of 5% oxygen for pure MnO_2 compared to those for MnO_2 calcined at different temperatures. It can be seen clearly from Figures 4.53-4.55 that introduction of gold caused the changing in the shape of TPD profiles of catalysts compared to that of pure MnO_2 powder without calcination. It can be seen that desorption temperature of first peak and second peak shifred (about 470°C and 540°C) to the lower temperature when gold was introduced and calcined at 300°C and 400°C. However, for calcination temperature of 500°C, 1^{st} desorption temperature did not decrease and 2^{nd} desorption temperature almost did not change. To clarify whether presence of gold or calcination temperature that caused decreasing on desorption temperarture, Figure 4.59 should be simultaneously compared to Figures 4.53-

4.55. It can be observed that it was the gold that cause the decreasing on desorption temperature because TPD profiles for pure MnO_2 calcined at both 300°C and 400°C were similar to that without calcination, so it can be implied that decreasing in desorption temperature would not be obtained unless gold was introduced. However, TPD profile of pure MnO_2 calcined at 500°C was changed when compared to that for pure MnO_2 with our calcination. Combination between 1st and 2nd peaks was obtained. This combination caused increasing and slight decreasing in desorption temperature of them respectively. It can be observed from Figures 4.53-4.55 that the decreasing on desorption temperature for both calcination temperature of 300°C amd 400°C was comparable. The combination of 1st and 2nd peaks was obvious but desorption temperature of first peak was not decrease to the lower temperature when catalysts were calcined at 500°C. Interestingly, for calcination temperature of 500°C, the combination of 1st and 2nd peaks for pure MnO_2 was slightly obvious when compared to that for the case of presence of gold. Third peak was more apparently obvious when gold was introduced. For the effect of increasing gold loading, trend for calcination temperature of 300°C and 400°C is similar. Higher gold loding caused the lower desorption temperature. For the calcination temperature of 500°C, higher gold loading caused the closed distance between 1st and 2nd peaks. These results showed that gold loaded on MnO_2 might influence adsorption and desorption properties of oxygen. It indicated that gold might interact with MnO_2 and modify the oxygen bond strength, so it can enhance desorption of oxygen to be easily occurred since peaks of desorption were shifted to the lower temperature when gold was introduced into MnO_2 and calcined at 300°C and 400°C. However, calcination temperature of 500°C was so high that desorption temperature was not decrease. Moreover, presence of gold caused reduction of kinds of active sites from 3 types to 2 types because of the combination of the 1st and 2nd peaks. As shown in Figures 4.53-4.55, for any given gold loading, an increase

in calcination temperature results in shifting of these two peaks to closer. An increase in gold loading enhanced the merging effect. At the highest gold loading of 1.40 wt.%, Au/MnO_2 calcined at 500°C had a single desorption peak at about 520°C. From the experimental results, it can be stated that the presence of gold and calcination temperature could affect the oxygen desorption property of Au/MnO_2 catalysts. Moreover, the effect of gold loading was much greater the one of calcination temperature on the oxygen desorption profiles.

Figures 4.60-4.62 illustrate the TPD profiles of 5% oxygen for a series of Au/Y_2O_3 catalysts calcined at different temperatures. At the lowest calcination temperature of 300°C and for any given gold loading, there were two desorption peaks appearing at 270°C and 490°C. When calcination temperature incraesed to 400°C, a single desorption peak occurred at 490°C. Interestingly, the highest calcination temperature of 500°C caused desorption peak to be disappeared. It might be the different structure of catalyst calcined at different temperature that caused the disappearance of desorption peaks when catalysts were calcined at high calcination temperature. Figures 4.63 and 4.64 showed that a higher gold loading did not affect the oxygen desorption property of the catalysts. The desorption temperature for any gold loading and any calcination temperature was approximately the same. Figure 4.66 shows that for pure Y_2O_3, an increase in calcination temperature affects significantly its oxygen desorption property. The desorption peak completely disappeared at a calcination temperature of 500°C. From the TPD results of Au/Y_2O_3 catalyst, it can be stated that and addition of gold could not enhance its oxygen desorption properties. The oxygen desorption property of Au/Y_2O_3 depended solely on Y_2O_3 support and calcination temperature.